SANDIA REPORT
SAND2012-9834
Unlimited Release
Printed November 2012

Ultrasensitive, Amplification-free Assays for Detecting Pathogens

Robert J. Meagher

Prepared by
Sandia National Laboratories
Albuquerque, New Mexico 87185 and Livermore, California 94550

Sandia National Laboratories is a multi-program laboratory managed and operated by Sandia Corporation, a wholly owned subsidiary of Lockheed Martin Corporation, for the U.S. Department of Energy's National Nuclear Security Administration under contract DE-AC04-94AL85000.

Issued by Sandia National Laboratories, operated for the United States Department of Energy by Sandia Corporation.

Available to DOE and DOE contractors from
U.S. Department of Energy
Office of Scientific and Technical Information
P.O. Box 62
Oak Ridge, TN 37831

Telephone: (865) 576-8401
Facsimile: (865) 576-5728
E-Mail: reports@adonis.osti.gov
Online ordering: http://www.osti.gov/bridge

Available to the public from
U.S. Department of Commerce
National Technical Information Service
5285 Port Royal Rd.
Springfield, VA 22161

Telephone: (800) 553-6847
Facsimile: (703) 605-6900
E-Mail: orders@ntis.fedworld.gov
Online order: http://www.ntis.gov/help/ordermethods.asp?loc=7-4-0#online

SAND2012-9834
Unlimited Release
Printed November 2012

Ultrasensitive, Amplification-free Assays for Detecting Pathogens

Robert Meagher
Biotechnology and Bioengineering
Sandia National Laboratories
P.O. Box 969, MS 9291
Livermore, CA 94551-0969

Abstract

Hybridization of nucleic acid probes has the potential to directly detect pathogens without requiring resource-intensive amplification steps, but conventional approaches to direct hybridization are typically slow or suffer from low sensitivity. In this work, we have characterized a novel approach for rapid detection of low-abundance nucleic acids by direct hybridization in solution, with sensitive analysis enabled by electrophoretic preconcentration of nucleic acids at a nanoporous membrane. We performed proof-of-concept testing of the assay using a model DNA virus, showing direct detection of as little as 400 amol (~240 million copies) with current (un-optimized) hardware. We extensively characterized the preconcentration process for DNA, and determined rates of preconcentration and efficiency of recovery as a function of preconcentration conditions, membrane formulation, and DNA size. The membrane preconcentration device also enables rapid, ultra-sensitive size-based separation of nucleic acids, and has been demonstrated for multiplex PCR analysis of drug resistance genes in bacteria.

ACKNOWLEDGMENTS

This work was funded by the Early Career LDRD program (project 149705).

I thank Anup Singh for helping con ceive the idea for this work, and Anson Hatch for addition al helpful discussions.

Some support with experim ents and laborator y equipment was provided by Num rin Thaitrong, Peng Liu, Ron Renzi, Mike Bartsch, Dan Yee, Jim Van de Vreugde, and Dan Throckmorton.

CONTENTS

FIGURES

TABLES

NOMENCLATURE

Abbreviations

NA	Nucleic acid
DNA	Deoxyribonucleic acid
RNA	Ribonucleic acid
PCR	Polymerase Chain Reaction
SDS-PAGE	Sodium dodecyl sulfate polyacrylamide gel electrophoresis
T_m	NA duplex melting temperature
TAPS	N-Tris(hydroxymethyl)methyl-3-aminopropanesulfonic acid (a buffer anion)
HEPES	4-(2-hydroxyethyl)-1-piperazineethanesulfonic acid (a buffer anion)
TTE	Tris-TAPS-EDTA (a common buffer for electrophoresis of DNA)
PDMA	Polydimethylacrylamide (a polymer sieving matrix for electrophoresis)
LPA	Linear polyacrylamide (used as a wall coating polymer to suppress electroosmosis)
c^*	Overlap threshold or entanglement threshold concentration (a property of a semi-dilute polymer solution used as a sieving matrix for macromolecules.

Reactive species

P	Probe
T	Target sequence
N	Non-target sequence(s)

Symbols (in equations and mathematical expressions)

C_i	Concentration of species *i*
[ ]	Terms in brackets (*e.g.* [P]) denote concentration of that species
k	Overall rate constant for hybridization, second-order.
k'	Nucleation rate constant for hybridization, second-order.
$t_{1/2}$	half-time for first-order reaction
t	time
x	Spatial coordinate
δ	Charateristic length scale
D_i	Diffusivity for species *i* (about 10^{-6} cm^2/s for a 20mer oligo; 4×10^{-8} for a 2.1 kbp dsDNA; [1])
μ_i	Electrophoretic mobility (about 4×10^{-4} cm^2/Vs for DNA [1])
E	Electric field strength (typically 20-400 V/cm in this work)
$\boldsymbol{E}$	Electric field vector
Pe	Peclet number for electrophoretic transport $Pe = \mu E \delta / D$
Da	Damköhler number $Da = k[\mathrm{P}]_0 \delta_T^2 / D_T$

1. INTRODUCTION

All techniques or assays for detecting the presence of *specific* nucleic acid (DNA or RNA) sequences in a sample require, at some point, hybridization (or base pairing) of a DNA (or RNA) "probe" or "primer" to its complementary target. Hybridization can be carried out in homogeneous (solution-phase) or heterogeneous (surface- or solid-phase) reactions. Detection of hybridization events (*i.e.* determining whether or not a probe has bound to its target) can be "direct", meaning the probe binding itself transduces a discernible signal, but frequently probe binding is used in combination with an enzymatic signal amplification process. The most familiar example of an enzymatic signal amplification is polymerase chain reaction (PCR), in which hybridization of a pair of primers directs enzymatic synthesis of DNA downstream from the priming site. PCR amplification proceeds exponentially, and repeated cycles of the reaction can produce $>10^9$ copies of an initially low-abundance target, allowing detection.

Although exceedingly powerful and ubiquitous in molecular biology, enzymatic amplification techniques such as PCR suffer from at least two drawbacks for use in fieldable or portable diagnostics:

(1) Complex samples (blood, soil, etc) frequently contain chemicals that inhibit the PCR reaction, and require cleanup, which adds complexity to the process, and

(2) Most enzymes require continuous cold storage until immediately before use for optimal activity.

Because of these perceived limitations of PCR and other enzymatic techniques for routine, portable nucleic acid detection, we sought to develop a novel assay for *direct* detection of hybridization of nucleic acids in a solution-phase assay.

Direct detection of hybridization (whether in solution or on surfaces) generally involves using a probe that is labeled with a fluorophore, radioisotope, or other label, and then using the label to track whether or not the probe is bound to a target. In surface hybridizations, this is easily accomplished by performing a "wash" step after hybridization, to remove unbound probes; any probe remaining after the wash can be presumed to be bound to a surface-immobilized target. However, surface hybridizations (compared to solution hybridizations) are often slow, requiring hours to approach saturation of targets. The kinetics of surface hybridizations are frequently influenced by mass transfer limitations as well as surface-related effects on secondary structure or availability of targets. Solution hybridizations can be driven to completion within seconds or minutes using high concentrations of probes, but there is no simple equivalent of a "wash" step, making it difficult to discern whether or not probes are bound to targets.

One approach to discerning probe binding in solution-phase hybridization is physical separation. Frequently, probe molecules are "small" (ranging from ~20-base long oligonucleotides to several hundred base polynucleotide probes). Targets, on the other hand, might be fragments of a bacterial or viral pathogen's DNA or RNA, and can be thousands of bases or more in length. Thus, a step capable of separating a sample into "small" and "large" fractions can be used to discern hybridization of probe: any probe that is detected in the "large" fraction can be assumed to be bound to a target. A second approach involves use of "quenched" (molecular beacon-type) probes, which consist of a dye and quencher pair which are separated through the process of hybridization. Although useful, quenchers are rarely 100% efficient, which limits the dynamic

range of targets that can be detected this way (a small amount of hybridized, unquenched probe may be difficult to discern in a background of quenched but still weakly fluorescent unbound probe).

In either case (physical separation, quenched probes, or approaches that combine the two techniques), a fundamental limitation exists on the ability to detect small quantities of probe after hybridization. Traditionally, extremely sensitive detection has been achieved by using radiolabeled probes (*e.g.* DNA labeled with ^{32}P), although due to safety considerations, use of radioactivity in the life sciences is decreasing, typically in favor of fluorescence techniques. To achieve ultrasensitive detection of fluorescent probe binding, we have coupled a physical separation process (microchannel electrophoresis) to a preconcentration step involving electrophoresis across a photopatterned nanoporous membrane.

1.1. Microfluidic preconcentration for hybridization analysis

We sought to employ electrophoretic preconcentration at a photopatterned, nanoporous "membrane" within a microchannel as a platform to accelerate hybridization of probe to target, and to increase target concentration prior to physical separation of bound and unbound probe, allowing detection by laser-induced fluorescence. Figure 1 illustrates the assay concept.

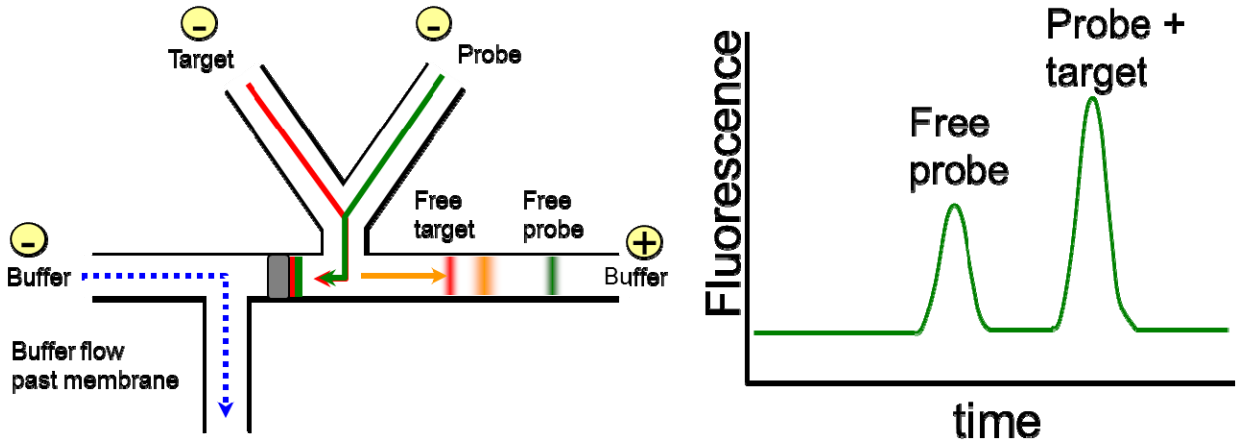

Figure 1: Concept of electrophoretic mobility shift assay to detect hybridization of a probe to a target. A target & probe are concentrated (sequentially or simultaneously) at a photopatterned membrane, where they mix together in a small (~nL) volume at high concentration. After incubation, the electric field is switched to send the analytes down a separation channel field with a sieving polymer, which allows separation of "free" probe (which is small) and "bound" probe hybridized to target (which is large). Laser-induced fluorescence (LIF) detection at a point downstream the separation channel detects separate peaks for the free probe and probe-target hybrid. The assay can also be performed with off-chip hybridization, in which case the the probe and target are pre-mixed & incubated off-chip, and subsequently loaded on chip, concentrated at the membrane, and separated as illustrated above.

This assay builds upon previous work with preconcentration of proteins at photopatterned membranes, for increasing the sensitivity of SDS-PAGE analysis [2] or for mixing antigen and

antibody for immunoassays, with native gel electrophoretic separation [3-5]. The hybridization assay is similar in concept to the mobility-shift immunoassay, except that a dye-labeled oligonucleotide probe binds to an unlabeled target DNA or RNA strand, as opposed to a dye-labeled antibody binding to an unlabeled protein target. Similar to the immunoassay, microchannel electrophoresis through a sieving matrix is used to separate bound and unbound probe, with the sieving matrix (in this case a semi-dilute polymer solution) causing a mobility shift between unbound probe (which is small) and probe bound to the target (which is large).

1.2. Description of work

In the course of this work, major effort was placed in characterizing the rate and biases of DNA preconcentration at photopatterned membranes, as this is a fundamental process underlying the proposed hybridization assay, as well as numerous other applications wherein we might wish to concentrate DNA or RNA to improve detection limits for an analytical separation or assay.

Experiments performed to quantify DNA concentration were performed with multiple sizes of DNA, with either neutral or negatively charged membranes, at a variety of preconcentration conditions (varying both field strength and time of preconcentration). The experiments and results are discussed at length in a peer-reviewed manuscript, Meagher and Thaitrong, "Microchip electrophoresis of DNA following preconcentration at photopatterned gel membranes", *Electrophoresis* 2012, 1236-1246 [6]. Also available online with this reference is an extensive set of supplemental information, giving additional details about experimental protocols, device performance, and analysis.

Following the detailed characterization of the preconcentration process itself, proof-of-concept assays were performed demonstrating the hybridization assay concept. For demonstration purposes, I used a model viral target, M13mp18, a circular single-stranded DNA virus of 7249 bases. Detection limits of ~400 amol were obtained, with relatively little optimization of the separation. Experimental limitations suggest additional areas for improvement, including methods to remove excess probe after hybridization but before separation; early exploration was made of some possibilities, including enzymatic digestion of excess probe.

In addition, given the success of the DNA concentration and separation (apart from the hybridization assay), the membrane preconcentration chip was tested for application in high-senstivity, high-resolution separation of PCR amplicons, specifically for the case of detecting genetic markers of drug resistance in bacteria. Although separate from the original intent of the PCR-free hybridization assay, this demonstration provides proof-of-concept using the membrane preconcentration device for analytical separations that could be an enabling feature of numerous assays.

Apart from the experimental demonstrations, theoretical considerations were used to determine optimal protocols for hybridization. The original intent had been to develop a detailed model of on-chip hybridization, for the sake of significantly accelerating hybridization. A closer look at the process suggested that hybridization on-chip, at least for the case of small oligonucleotide probes, offers relatively little benefit and a host of complicating factors, relative to off-chip hybridization. However, experimental observations and modeling were used to develop some

insights into what is occurring on the chip near the membrane, and how this might affect hybridization.

2. THEORETICAL ANALYSIS

2.1. Thermodynamics and kinetics of hybridization

Nucleic acid hybridization is fundamentally an equilibrium reaction. Literature on both the thermodynamics and kinetics of this reaction is summarized in the review by Wetmur [7]. For the case of a probe, P, binding to a target, T, in presence of a mismatched, or non-target strand, N, we can consider two separate equilibria: probe binding to target (PT) and probe binding to non-target:

$$P + T \leftrightarrow PT \qquad (1)$$

$$P + N \leftrightarrow PN \qquad (2)$$

The free energy (and thus equilibrium constants) for these reactions are determined by the degree of complementarity between the probe and the target or non-target. Besides degree of complementarity (perfect base-pairing vs mismatches), numerous factors influence stability of the duplex, including concentrations of monovalent and divalent cations, denaturants such as urea or formamide, and temperature, as well as concentration of the probe and target. In case of a dilute target with a probe in excess, the melting temperature (T_m) is generally defined as the temperature at which half of the target is bound to its complement. Numerous online tools are available to determine T_m for a given probe/target combination as a function of solution conditions, *e.g.* the OligoAnalyzer tool from Integrated DNA Technologies (www.idtdna.com) [8, 9]. Additional tools for comparing thermodynamic stability of probe-target and probe-mismatched target combinations (although restricted to DNA probes with RNA targets) are available from MathFISH (http://mathfish.cee.wisc.edu/) [10].

Given the experimentally determined variables of temperature, salt concentration, and denaturant concentration, it is typically possible to find conditions that give high binding of probe to target (large fraction of target with probe bound), with low binding of probe to non-target. Conditions that maximize target binding while minimizing non-target binding are referred to as "high stringency". Stringency increases with increasing temperature, increasing denaturant concentration, or decreasing cation concentration. The condition of high stringency essentially defines a thermodynamic "objective" for hybridization; the remaining task for optimization is to determine conditions that meet that objective while maximizing the kinetics or rate of hybridization. Table 1 summarizes the effects of various experimental parameters on both the thermodynamics (expressed as T_m of a duplex) and kinetics of hybridization.

Table 1: Influences of experimental parameters on thermodynamics and kinetics of nucleic acid duplex formation

Variable	Thermodynamics: effect on duplex stability (T_m)	Kinetics: effect on rate of duplex formation
Mismatched bases	- -	minimal
Monovalent cations (Na^+, K^+)	+	+
Divalent cations (Mg^{++})	+	++
Concentration of probe/target	+	++
Temperature	-	+ or -
Denaturants (urea, formamide)	-	Slight -

Presuming that hybridization conditions are chosen to provide a high degree of probe binding to target (equilibrium lies far to the right of reaction 1), and a low degree of probe binding to non-target, the rate of hybridization reaction 1 can be described as follows:

$$\text{Rate} = d[PT]/dt = k[P][T] \qquad (3)$$

Since hybridization follows second-order kinetics, it is reasonable to believe that simultaneously increasing both probe and target together at the membrane will accelerate the hybridization. The original concept of this assay relies on this effect to speed a hybridization that might otherwise take hours down to a few minutes. However, in solution-phase hybridization, and particularly in the case we are interested in of detecting a low-concentration target, the probe is typically in excess. This is easily achievable with synthetic oligonucleotide probes: for purposes of a microliter-scale hybridization, sufficient dye-labeled probe for thousands of assays can be synthesized for ~$100. As long as the probe is in sufficient excess (*e.g.* 10-fold relative to target), the "free" probe concentration does not change substantially even as the reaction progresses toward complete saturation of the target, and hence the reaction follows pseudo-first-order kinetics:

$$\text{Rate} = d[PT]/dt \sim k[P]_0[T] \qquad (4)$$

With pseudo-first-order kinetics, a host of familiar conclusions can be deduced, for example the half-time for the reaction (the time required to achieve probe binding to half of the initial population of target strands) is given by:

$$t_{1/2} = \ln 2 / k[P]_0 \qquad (5)$$

In the case of excess probe, the time required to achieve half (or ¾, or 90%, etc) coverage of the target is *independent* of the target concentration. For syntetic oligonucleotide probes, the probe concentration is an easily controlled parameter, and probe can *always* be used in excess of a low-copy number target. This is also requirement if *quantitation* of the target is desired: if the target is in excess, and binds with all available probe, it is impossible to determine the total target concentration. With this simple consideration, the rationale for accelerating hybridization at the membrane disappears. Hybridization can be performed "off chip" (*i.e.* in a test tube and incubator), and then the power of the preconcentration chip is used to increase the concentration of both probe and target to improve the detection limit during the separation step.

Performing the hybridization off-chip greatly simplifies the choice of hybridization buffer, as well as the modeling of the hybridization process. As mentioned in Table 1, hybridization kinetics are strongly dependent upon concentration of both monovalent and divalent cations. To achieve predictable hybridization on a chip at a membrane, we would need to have a good idea of the ionic conditions at the membrane. In general, applying an electric field across a semi-permeable membrane can result in local changes in the ionic composition, and thus we would need a good prediction of the local (as opposed to overall) buffer condition at the membrane. This is, in principle, predictable, as will be described in Section 2.3.1.

The kinetic effect of monovalent cations on the rate of hybridization in solution is reviewed in Reference [7]. Briefly, the second-order rate constant k (units M^{-1} s^{-1}) is given by the relation:

$$k = k' L^{1/2} / N \qquad (6)$$

In this equation, k' is a nucleation rate constant, which is a monotonically increasing function of salt concentration. L is the length of the shortest strand participating in the hybridization, and N is the "complexity", defined as the number of non-repetitive bases in the shortest strand. In the case of a short, non-repetitive oligonucleotide, the complexity N equals the length L, and thus:

$$k = k' L^{-1/2} \qquad (7)$$

The nucleation rate constant k' can be generalized as:

$$k' = (4.35 \log_{10}[Na^+] + 3.5) \times 10^5 \qquad (8)$$

for $0.2 \le [Na^+] \le 4.0$ M

For the case of a 20mer oligonucleotide, we can calculate the rate constant, and thus the time scale for hybridization, as a function of salt concentration and probe concentration (two easily controlled experimental parameters). The results are plotted in Figure 2 below. Data are extrapolated to salt concentrations below the range given for k' (dashed portion of curves). Although the extrapolation may not be accurate, the key point is that particularly at low concentrations, the hybridization rate is a strong function of salt concentration: the apparent slope at $[Na^+] = 0.2$ M suggests that the time scale for hybridization scales roughly as $[Na^+]^{2.7}$. Hybridization at low salt concentrations are *very* slow, even with large excess of probe.

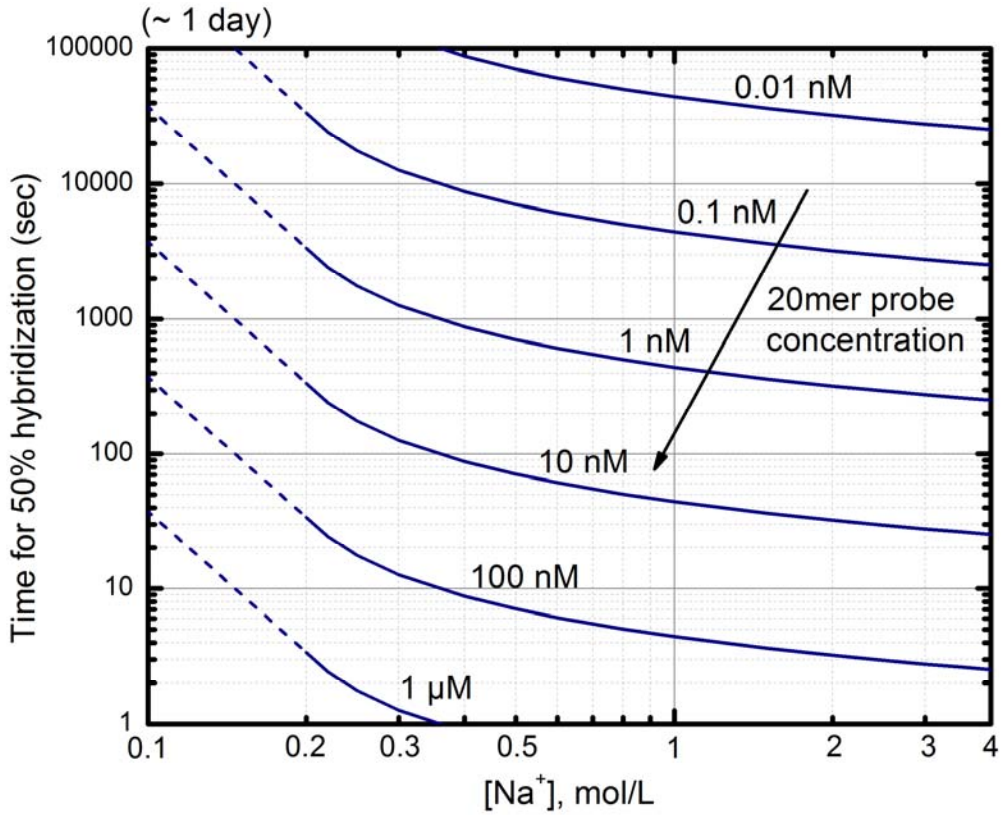

Figure 2: Characteristic time scale for hybridization of an oligonucleotide probe (in excess) to a target in solution, as a function of cation concentration. Based on Reference [7].

2.2. Selection of buffers for hybridization and electrophoresis

Electrophoresis works best with relatively low conductivity buffers, which is clearly at odds with the trends in Figure 2. For a given electric field strength, high conductivity buffers lead to high currents, resistive heating, and reduced quality of separation. On a practical level, high conductivity buffers also result in increased rates of electrolysis, generation of bubbles, and a higher likelihood of a failed run (*e.g.* due to a tiny bubble blocking a microchannel). Conductivity of a buffer is directly related to the electrophoretic mobility or "speed" of the ions in the buffer, as well as the total concentration of each ion. The cations which facilitate hybridization, namely Na^+, K^+, and Mg^{++} (and presumably similar monovalent and divalent metal cations), are "fast" ions, and not the best choice for stable electrophoresis. These ions can be used, but concentrations must be kept fairly low (*e.g.* $[Na^+] < 25$ mM). Better cations for electrophoresis include weak bases with lower mobility, such as Tris, bis-tris-propane, and similar: larger molecules which are only partially ionized at the pH of the buffer, leading to a low effective mobility. Electrophoresis can thus "tolerate" a somewhat higher concentration of these cations, *e.g.* [Tris] < 100 mM. The very character that makes these ions a good choice for electrophoresis (large size and partial ionization) also makes them poor at facilitating nucleic acid hybridization. Cation effects on hybridization are due to hydrogen bonding and charge screening interactions with the ribose-phosphate backbone of nucleic acids, and larger cations are simply not as effective as smaller cations in this role [11].

Divalent cations (typically Mg^{++}) can have a dramatic effect on both kinetics and duplex stability at relatively low concentrations (<10 mM) [8], and thus can presumably be used in buffers that are simultaneously compatible with electrophoresis, and also facilitate hybridization. As a practical matter, Mg^{++} must be added in the form of a salt with a high-mobility anion such as Cl^-, SO_4^{2-}, or H_3COO^-. This is non-ideal: in the case of DNA electrophoresis, the background electrolyte should generally contain anions of lower mobility than DNA anions; otherwise electrophoresis is primarily working to move the "fast" ions (*e.g.* Cl^-). Typical buffer anions for electrophoresis of DNA are TAPS, borate, or HEPES. Sufficiently high concentrations of Mg^{++} may form insoluble precipitates with these anions.

Historically most studies of hybridization kinetics avoid use of divalent cations because nucleases (DNAses and RNAses) typically require a divalent cation as a cofactor. Including divalent cations in an extended hybridization can thus inadvertently lead to destruction or digestion of target nucleic acids. A large body of data is available on the kinetics of nucleic acid hybridization in presence of monovalent cations (typically Na^+ or K^+, which have roughly equivalent effect). Although divalent cations are known to accelerate hybridization, comprehensive, quantitative data are not present in literature. Empirical correlations are sometimes used; for example a "typical" PCR buffer containing 50 mM K^+ and 1.5 mM Mg^{++} is described as being "equivalent" to 200 mM Na^+, in terms of the kinetic effect on hybridization [7].

In practice, two strategies appear to work well for performing off-chip hybridization assays that are compatible with electrophoresis: (1) a buffer comprising a fairly high concentration of the sodium salt of a "good" anion for electrophoresis (e.g. ~300 mM Na^+, 380 mM HEPES, with a pH of about 8), or (2) a "PCR"-like buffer, comprising 50-100 mM NaCl, plus 1.5-2.0 mM $MgCl_2$. In either case, the best results for electrophoresis require the hybridization buffer to be diluted 5-10-fold into DI water or running buffer in the sample well, to avoid a drastic conductivity mismatch between the sample and the buffer in the microchannel. One option that remains to be explored is a "PCR"-like buffer with a low-mobility anion (*e.g.* sodium-HEPES) supplemented with $MgCl_2$: such a buffer system might allow hybridized samples to be injected directly into the device with no dilution or at least less dilution than the higher-conductivity buffers previously tested. Diluting 5-10-fold (from ~0.3M Na to ~30 mM Na) does have the advantage of drastically slowing down the hybridization, such that hybridization is not progressing during the course of the on-chip analysis, and reduces the importance of carefully maintaining the chip at the same temperature as the hybridization reaction.

2.3. Modeling of on-chip hybridization

As described above, in the case of hybridization of an oligonucleotide probe, there is little apparent advantage to performing hybridization on a chip at a membrane, versus performing the same hybridization off-chip and then simply using the membrane to increase the concentration for the sake of improving detection limits during electrophoresis.

Should a situation arise where on-chip hybridization *is* desirable, several considerations arise for modeling.

(1) What is the concentration profile of "probe" and "target" near the membrane?
(2) What is the salt concentration near the membrane?
(3) What is the specific rate of formation of probe + target hybrids?

Basic conservation of mass allows us to describe the concentration of each charged species at a membrane, with simultaneous solution-phase reaction. For a one-dimensional simplification of the microchannel and membrane, the equation governing the time- and position-dependent concentration of species *i* is:

(9)

where C_i is concentration, D_i is diffusivity, μ_i is electrophoretic mobility, E is the electric field strength, and $R_{v,i}$ is the volumetric rate of the hybridization reaction. The species (*i*) to be considered include the probe(s) as well as all target and non-target strands; the simplest case would include just two species: one probe and one target. The time-course of accumulation only (without reaction) for a single species is illustrated schematically below. Each analyte has a "bulk" concentration (*i.e.* in the reservoir) of $C_{i,0}$. Appropriate initial & boundary conditions would be:

(10a)
(10b)
(10c)

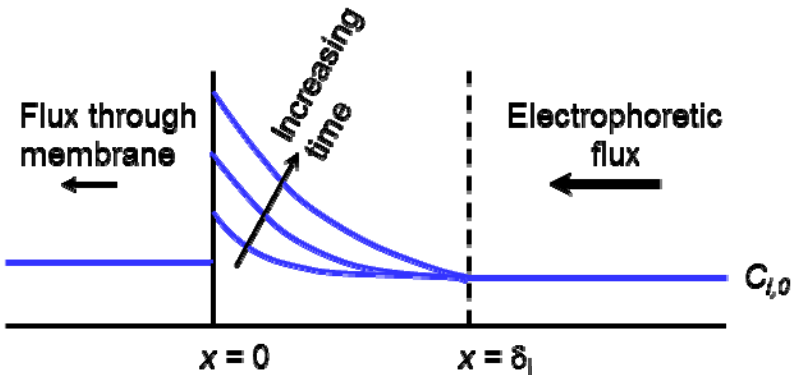

Figure 3: Accumulation of a single species at a semi-permeable membrane (with no reaction).

In other words, accumulation is occurring in a "boundary layer" of thickness δ near the membrane; the boundary layer thickness δ is potentially different for each species, depending, *e.g.* on the diffusivity of the species. Species may also penetrate through the membrane; this is described by the final boundary condition with a "leakage" coefficient α, which is also species-dependent (*i.e.* large species are more likely than small species to diffuse through the membrane). Solution of this system including the homogeneous reaction and the non-constant

flux boundary condition at $x = 0$ is not trivial, and (to the best of my knowledge) requires numerical techniques.

Some simplification can be obtained by dimensionless analysis, *e.g.* the electrophoretic Peclet number, $Pe = \mu_i E \delta_i / D_i$ is likely to be large (>100) using typical values of μ and D for DNA (4×10^4 cm^2/Vs and 10^{-7} cm^2/s, respectively [1]), length scale δ on the order of 100 μm (similar to channel diameter, and similar to the distance from the membrane to the channel intersection with the sample inlet), and E on the order of 60 V/cm. This would indicate that diffusion is relatively less important than convection in establishing the concentration profile over a "fixed" length scale on the order of the channel diamter. Alternatively the relevant length scale δ over which both convection and diffusion are both "interesting" is defined by setting Pe ~ 1; *i.e.* choose $\delta_i = D_i/\mu_i E$. In general the electrophoretic mobility μ of DNA is relatively independent of size, whereas the diffusivitiy D is a decreasing function of chain length L (for long chains, $D \sim 1/L^m$, where the exponent m is on the order of ½ to 3/5, depending on the specific solution conditions [12]). Thus for a given electric field strength, we can predict that the length scale $d_i \sim 1/L^m$.

We can also define a Damköhler number describing the relative importance of reaction and transport. For the case of a simple two component system (probe P and target T) where the probe has a "bulk" concentration of 10 nM (assumed to be everywhere larger than the target concentration), $Da = k[P]_0 \delta_T^2 / D_T$; using information in Figure 2, *e.g.* for the case where [P] ~ 10 nM and [Na^+] = 0.3M, $k[P]_0 \sim 83$ s^{-1}; we can infer that the consumption of target is "fast" relative to diffusive transport [$Da \sim 10^3$]. In other words: if the reaction were truly second-order (and not pseudo-first order with a large excess of probe everywhere), the actual concentration profile of the target and probe would matter.

2.3.1. Ion concentration polarization

Answering question (1) involves considering the phenomenon of ion concentration polarization when an electric field is applied across an ion-permselective membrane. When a membrane is not completely permeable to buffer ions (meaning transport across the membrane is restricted, relative to transport in free solution), or if the membrane preferentially allows passage of ions of a certain charge (*e.g.* a cation or anion-exchange membrane), ions of one charge accumulate on one side of the membrane. Counterions must also accumulate to maintain local electroneutrality, although there may be a very thin boundary layer near the membrane where this breaks down, and electroneutrality can also be maintained through acid-base equilibria (dissociation of water into H^+ and OH^-), which would result in a pH change. On the opposite side of the membrane, ions are depleted. This phenomenon has been known for decades, stemming back to interest in electrodialysis for water desalination, and this has been an interesting process for theoretical analysis of transport phenomena [13-15].

Interest in this field has been renewed with the advent of microfluidic devices involving electrokinetic concentration across nanoporous membranes, or at microchannel-nanochannel junctions [16-20]. Recent applications of the theory to the specific case of microfluidic preconcentration devices (building, of course, upon decades-old transport analysis) have been published [21, 22], and summarized in a tutorial review by Zangle *et al* [23].

Among the highlights of this review are models predicting the location (if any) of a concentrated zone of "analyte" (in our case, DNA), as well as features of the ion concentration polarization. Multiple regimes are possible depending on specifics of the device (surface properties, buffer properties, *etc*). The salient feature of ion concentration polarization that appears to apply to the our preconcentration device is that, upon applying an electric field, buffer ions "polarize" (accumulate & deplete) adjacent to the membrane. This disturbance propagates as a shock through the micrcodevice in the direction of the applied field. There is a discontinuity in buffer ion concentration at the boundary of the shock, but the ion concentration behind the boundary (i.e. near the membrane) remains stable over time as long as the electric field is maintained. This situation is illustrated in Figure 4. Prior to application of the electric field, salt concentration throughout the device is uniform. Upon applying the electric field, the salt concentration reaches new equilibrium values on either side of the membrane. The boundary between the zones at the new equilibrium and the original (bulk) salt concentration advances with time.

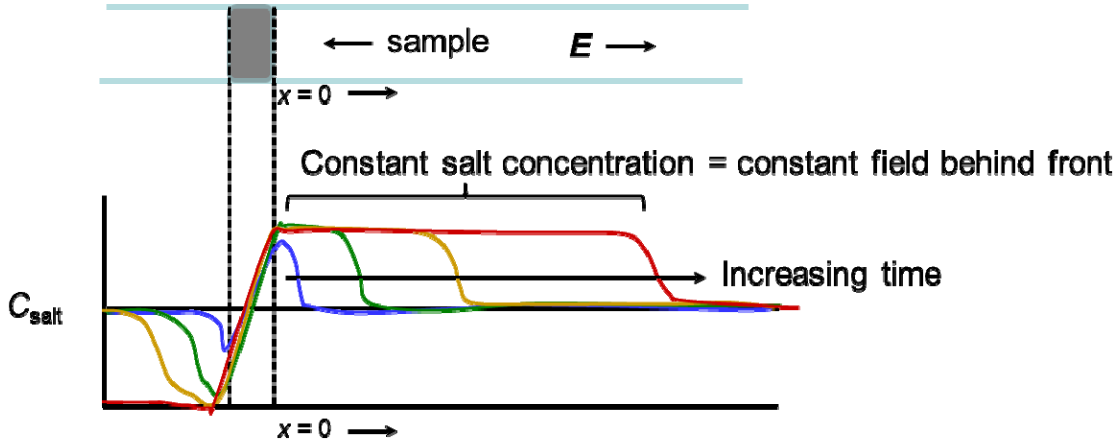

Figure 4: Evolution of concentration polarization upon applying an electric field across a nanoporous membrane in a microchannel, in the case of negligible electroosmotic flow in the microchannel.

This prediction is useful from the standpoint that it removes the necessity of explicitly modeling the buffer ion transport in addition to DNA transport and hybridization kinetics. Rate constants for hybridization can be calculated directly from the prevailing salt concentration near the membrane, which remains constant shortly after application of the field.

The difficulty with this predictive model is that several of the parameters that appear explicitly in the calculation of the new equilibrium salt concentration are not known with certainty for the case of a photopatterned gel membrane. Specifically, the model requires knowledge of the pore size and surface charge density of the membrane, and the zeta potential of the microchannel surface.

In our experiments, we examined two cases: a "neutral" polyacrylamide membrane (made of polyacrylamide and bisacrylamide), and an "an ionic" polyacrylamide membrane supplemented with acrylic acid as a co-monomer during polymerization. The actual pore structure of a polyacrylamide gel is difficult to discern, with different methods (including electron microscopy techniques) yielding conflicting results [24-28]. From literature, we can estimate that the

average pore size of a 40%T, 10%C must be on the order of 1-2 nm. We can also estimate the total number of charged groups present, based on the known starting concentration of acrylic acid. We can thus treat the membrane as a bundle of uniform, parallel nanochannels with diameter equal to the average pore size, with a known amount of total charge localized to the surface of those nanochannels, and thereby get a reasonable estimate of surface charge density to feed into the model. In the microchannel segment, the channel surface is coated with linear polyacrylamide (LPA) to suppress electroosmotic flow. We do not routinely measure zeta potential of our devices. Prior work has shown that, if the coating is properly applied, the zeta potential of an LPA-coated microchannel is indistinguishable from zero [29], within the precision of the measurement. This is the desired outcome of the coating (complete suppression of EOF), but unfortunately leads to a singularity (division by zero) in computation of the equilibrium salt concentration. In reality, the zeta potential is not identical to zero, but rather has a small but finite negative value. Since we can not measure this value with any precision, we can not calculate the equilibrium salt concentration with any precision.

In the case of a truly neutral membrane, the model would predict zero concentration polarization (salt concentration remains the same as the initial salt concentration after the field is applied). In reality, a small percentage of acrylamide is always hydrolyzed to acrylic acid, so a small amount of charge is present, and thus some degree of concentration polarization is likely. In the case of a "strongly charged" membrane fabricated with 0.1M acrylic acid, and fudging a small (but non-zero) zeta potential (1 mV) the model predicts a new equilibrium buffer concentration (for a Tris-TAPS buffer) of ~ 1 mol/L. This is exceedingly high, and approaches the solubility limit of the TAPS anion (ion solubility is not considered in the transport model). Given the uncertainty in the actual value of the zeta potential, it is fair to say that an anionic membrane results in strong concentration polarization, perhaps by an order of magnitude, but it is difficult to predict the exact concentration, and thus difficult to use correlations like Figure 2 to predict actual rate constants.

Given the difficulty in measuring device properties to predict salt concentration, it would be useful to devise an experimental technique to infer salt concentration. One possibility would be to monitor conductivity near the membrane, *e.g.* with a pair of microfabricated electrodes connected to a high-impedance circuit. A second approach, which was tested but not fully developed, was to use a salt-sensitive dye, the collisional quencher 6-methoxy-N-(3-sulfopropyl)quinolinium (SPQ). SPQ is normally fluorescent (excited by long UV, with blue emission), but its fluorescence is quenched in a concentration-dependent fashion by collision with ions in solution. SPQ is an attractive molecule for this purpose because it is zwitterionic over a wide pH range [30], and has no apparent electrophoretic mobility. It is most sensitive to halide ions such as Cl^-, but also displays some sensitivity to electrophoretic buffer ions such as TAPS, and (weakly), to Tris [31]. Initial tests with SPQ indicated a decrease in fluorescence, and thus an accumulation of buffer ions, during preconcentration, but quantitation was difficult for two reasons: (1) The dye itself photobleaches quickly, necessitating the use of short exposures at low lamp intensity, and (2) the dye intensity displays some dependence on pH, and it is difficult to disentangle buffer ion concentration effects from pH shifts that may be occurring. The SPQ imaging technique does appear promising, and may be useful for further basic research characterizing ion concentration polarization during membrane preconcentration, particularly if combined with an orthogonal pH-sensitive dye.

2.3.2. DNA transport and accumulation at a membrane

Our manuscript published in 2012 describes detailed experiments measuring the rate of concentration of different sizes of DNA at neutral and negatively charged membranes, using both quantitative imaging of the concentration process as well as electrophoretic separation of DNA "ladders" following concentration [6]. From this work we can draw some useful conclusions, that allow us to make predictions about the *total accumulation* of DNA at a membrane, as a function of membrane type, DNA size, and preconcentration field strength.

- Small (20mer oligonucleotide) DNA passes through a neutral membrane without significant accumulation outside the membrane, even at low applied fields.
- Larger DNA (100-2000 bp) accumulates approximately linearly with respect to time at both types of membranes, with rate roughly proportional to electric field strength up to ~150 V/cm.
- At higher electric field strengths, smaller DNA (100 bp) enters the membrane and is not quantitatively recovered upon reversal of the field.

An additional, and important, conclusion, is that the neutral membrane overall provides a higher degree of preconcentration versus the negative membrane, and provides more reproducible results as well as better quality of separation over most of the range of parameters tested. The most likely explanation is deleterious effects of stronger ion concentration polarization at the charged membrane. Accumulation of excess ions leads to a drop in the effective field in regions of high ion concentration, slowing preconcentration. Reversal of the field upon injection also results in rapid shifts in the ion gradients, leading to un-stacking of concentrated bands, with broader peaks during the separation. This suggests that for optimal preconcentration, hybridization, and separation, a neutral membrane is more useful.

Imaging also provides some insight into the *spatial distribution* of DNA at membranes, as a function of membrane type, DNA size, and preconcentration field strength. Representative images are shown in Figure 5.

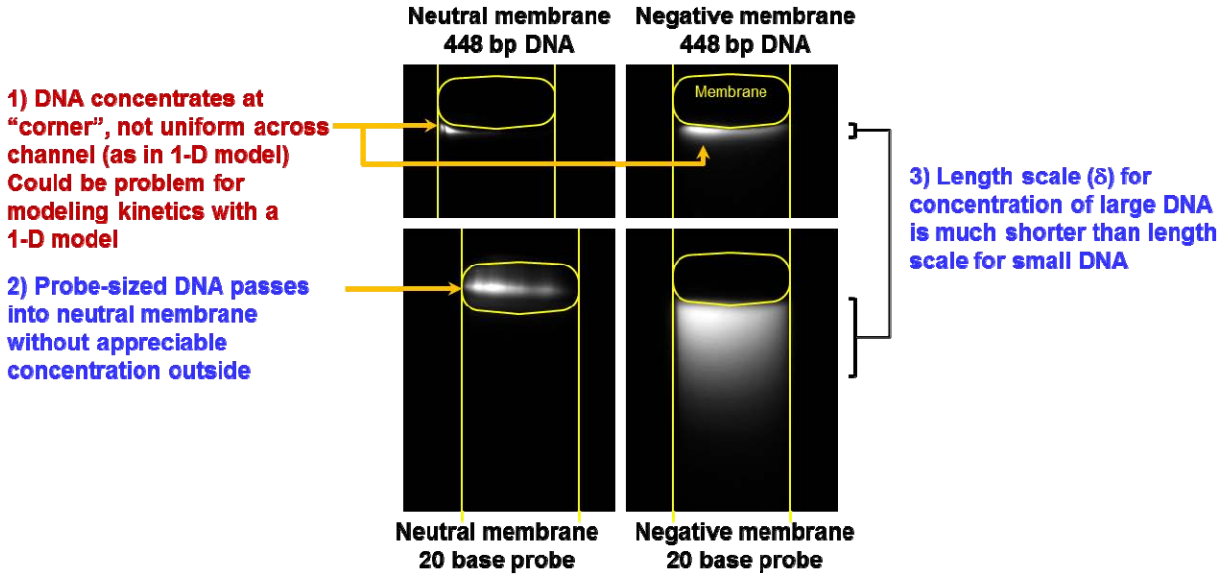

Figure 5: Patterns of DNA concentration observed during preconcentration at 63 V/cm across two types of photopatterned membranes (40%T, 10%C polyacrylamide; neutral or 0.1M acrylic acid), using dye-labeled DNA of different sizes (20 base ssDNA, or 448 bp dsDNA, labeled with Cy3).

These imaging experiments provide some further insights into the modeling problem:

- As predicted, the length scale over which conc entration occurs is longer for short DNA, although a detailed study of δ versus chain length has not been carried out.
- Concentration is not uniform across the widt h of the m embrane, due to the non-unif orm cross-section of the m embrane. The concentra tion profile is not strictly 1-D, and also varies from one device to the next (depending on the exact shape of the membrane).
- On the neutral membrane, which is predicted to be most useful overall, probe DNA is not effectively concentrated within the lim its of detection of the cam era, meaning that the concentration of probe can be treated as constant over the *entire* length scale.

The last observation, in partic ular, greatly simplifies the m odeling problem. Provided that the probe always remains in excess to the target everywhere, the process can be modeled as a simple well-mixed, fed-batch reactor, in which we only need to track the total accumulation of target as well as the rate of reaction with probe.

Subsequent experiments with pr econcentration and separation do not c ompletely agree with the observation of probe passing through the ne utral membrane with no concentration (*i.e.* we get a larger probe peak if we concentr ate for a long er time). In this ev ent, we can make use of the observation of the longer length scale for concentra tion of the probe, versus the target. Over the length scale wher e the target accumulates significantly, the probe has effectively constant concentration. If the probe concentration is al ways significantly larg er than th e target, we can again model the p rocess as a well-mixed fed-batch reactor, but we m ust track the total target accumulation as well as the probe co ncentration (and specifically, the probe concentration in the thin region near the membrane where the target is concentrated).

In either of these cases (with or without accumulation of probe), the problem is greatly simplified in that we don't need to model or predict the concentration profile of all species; just of the probe (in the case where the probe accumulates).

Note that these simplifications are only possible if concentration of the target in a corner does not lead to a situation where the target locally approaches or exceeds the probe concentration; in this case both concentration profiles must be determined to predict the rate of formation of hybrid. The problem is, of course, also complicated greatly if we cannot make accurate predictions of kinetic rate constants (as discussed in Section 2.3.1, it is difficult to make accurate predictions of buffer ion concentration).

2.4. Predicting assay performance and choice of targets

During testing of DNA concentration behavior, it was determined that a discernible peak could be observed starting with a single-dye-labeled DNA target at a concentration (in the reservoir on the chip) of 1 pM. This provides a starting point for predicting the detection limits for this assay, with the current configuration (same LIF detector, same membrane, same channel geometry, etc). Essentially, to see a target peak we need to have, in the reservoir, at least 1 pM of fluorophore bound to the target. This could be, *e.g.* 1 pM of target with 1 single-labeled probe bound to it, 100 fM of target with 10 single-labeled probes, or alternatively 100 fM of target with a single probe carrying 10 labels, *etc*. The key requirement (for the current device configuration) is that the product of (target concentration) × (dyes per target) > 1 pM.

In general, targets are "large" and have the opportunity to bind multiple probes, or long probes with multiple labels. However, this approach may not be feasible when only a few regions of the genome distinguish a virulent pathogen from an innocuous near neighbor. For example, bacterial pathogens have genomes on the order of a few megabases, but virulence may be associated only with a few genes. Those genes may be (a) variable in sequence across isolates (making it difficult to target with a synthetic probe), or (b) have regions that are homologous to genes from non-pathogens, meaning that we would need to further restrict our choice of targets only to regions that unique to pathogenic strains.

A second consideration that dictates the detection limit of a *pathogen* (virus particle or bacterial cell), as opposed to a "target", is the copy number of target per cell. In general, an intact viral particle contains one copy of the viral genome, and thus genome copy number and pathogen number are the same. A bacterial cell contains roughly one copy of the genome (depending on the state in the cell cycle). Most genes are represented only once in the genome, although some (like rRNA genes) may be represented a few times (typically less than 10). Some plasmids, particularly small ones, may exist in higher copy number, although larger plasmids are typically low copy number (1-10 per cell).

Bacterial genes may also be represented as RNA transcripts. In general the copy number of rRNA far exceeds any individual mRNA transcript: an actively growing cell may contain $>10^4$ copies of rRNA, making this an attractive "naturally amplified" target for hybridization. However, rRNA, due to its highly conserved nature across all phyla of bacteria, has relatively

poor discriminating power, particularly at the strain level. For example, *E. coli* O157:H7, *Shigella*, and non-pathogenic strains of *E. coli* are highly similar at the level of 16S rRNA, making discrimination by probe hybridization difficult. mRNA present another possible target, although except for "housekeeping" genes, bacterial expression of mRNA is unpredictable, and transcripts have short half-lives (on the order of minutes), meaning that copy numbers can be very low (*i.e.* may fluctuate between 0 and 1 copies).

Another possibility for both viral and bacterial targets is the possibility of whole genome probing, in which a large collection of probe molecules is used which, taken together, represent large portions of the genome, and bear many fluorescent labels. This approach offers the best possibility for highly sensitive detection. However, such probes are difficult to generate and use in very high concentration, leading to concerns with kinetics (conventional approaches would involve overnight hybridization, or use of PEG or other "crowding" agents to accelerate hybridization). The mosaic nature of bacterial genomes, with some highly conserved regions, might seem to limit this approach, although variants of this approach such as "checkerboard" hybridization have been used with some success to characterize clinical isolates (although this requires a long time and a large amount of DNA).

Based on the considerations of detection limits and target and probe multiplicity, we can generate a "detectability diagram", specific for the current device configuration.

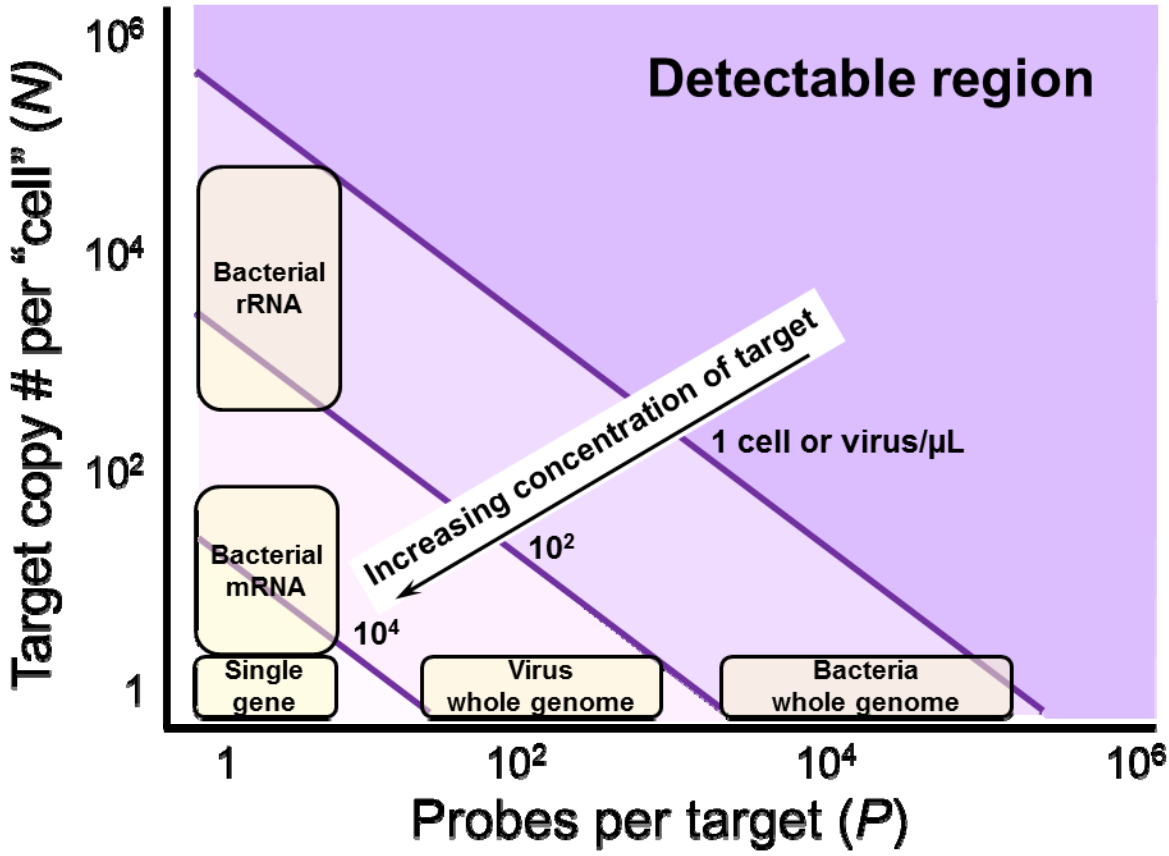

Figure 6: Detectability diagram for hybridization assay using the current chip and current detector, which has a demonstrated practical detection limit of 1 pM of single-dye-labeled DNA. For a given target concentration (*i.e.* the diagonal lines representing 1, 10^2, or 10^4 cell or virus/µL), the target is, in principle, detectable if using a combination of probe multiplicity *P* and target multiplicity *N* that lies above and to the right of the target concentration curve.

Figure 6 suggests that the assay, in its current form, will have difficulty detecting pathogens directly in clinical samples. Pathogen copy number varies widely depending on the nature of the pathogen, and the type of sample, over at least 12 orders of magnitude. For example, salmonella may be present at <1 organism per 10 mL of blood, making this an extremely challenging agent to detect by any means (including culture or PCR) without some form of macro-volume concentration. At the high end, influenza virus can reach peak concentrations of 10^9 genomes per mL of nasopharyngeal aspirate; Dengue virus can approach similar concentrations in blood, and Norovirus can approach 10^{11} copies per gram of stool. However, these represent the high end for each of these pathogens, and would put them barely within reach of this assay. This does not consider any dilution that occurs in adding hybridization reagents, or in transferring the assay to the chip (usually 5-10 fold dilution factor). Clearly to be useful, our direct hybridization assay would need to be coupled to a nucleic acid extraction "front-end" that can concentrate nucleic acids from a dilute sample into a concentrated microliter-scale volume. Approaches to accomplish this are currently under development through other projects at Sandia, including an LDRD-funded biosurveillance project (PI Steve Branda), and externally-funded human forensics project (PI Mike Bartsch), and the hybridization assay may be useful in combination with these techniques.

2.4.1. Advantage of FISH and flow cytometry for detecting intracellular targets

In parallel with this project, with the NIH-funded "FISH-n-Chips" project, we demonstrated that we could use FISH targeting the 16S rRNA to detect as few as ~10 cells by hybridizing probes to targets in *intact* cells, and then counting labeled cells in a microscale flow cytometry device (μFlowFISH) [32]. This presents a certain advantage over the purely solution-phase assay. The intact cell acts is a natural container that keeps the RNA target confined to a small volume (~1-2 fL for a bacterial cell), both during hybridization and detection, allowing us to perform detection in a "counting" or "cytometry" mode with hydrodynamic focusing. This provides better detection limits than we could achieve in electrophoresis where we are detecting bands of "free" RNA molecules released from lysed cells. RNA in solution is subject to the usual constraints of diffusional band broadening. Furthermore, molecules in solution freely fill the entire cross section of the microchannel, and thus many of them are simply not detected: the laser for LIF detection is focused to a small spot at the center of the channel, and does not interrogate the full cross-section of the channel. In FISH with flow cytometry the cells with intact RNA are hydrodynamically focused at the center of the channel which ensures that essentially every probe molecule in every cell passes through the detection volume.

3. HYBRIDIZATION ASSAY PROOF OF CONCEPT

Proof-of-concept was demonstrates with M13mp18, a closed-circular single-stranded DNA virus of 7249 bases in size. DNA from this virus was obtained in purified form from New England Biolabs. Assay performance is not expected to vary significantly with other types of virus (linear vs circular, single vs double stranded, DNA vs RNA). NA is denatured prior to hybridization, which would release DNA or RNA from an intact viral particle (as opposed to purified NA). Presuming a low starting concentration of viral DNA, re-annealing of a double-stranded genome is not expected to compete significantly for probe binding sites, although partially-rehybridized genomes could be problematic. RNA viruses might also be problematic from the standpoint of rapid degradation of the viral RNA once released from the intact viral particle, although the denaturing step will partially inactivate any nucleases (RNAse) that happen to be present, and absence of divalent cations will also reduce RNase activity. A reducing agent (dithiothreitol or 2-mercaptoethanol) or RNAse inhibitors can also help block RNAse activity; these additives were not tested in the current work.

The M13 assay is illustrated schematically in Figure 7 below, along with data illustrating an actual assay separation.

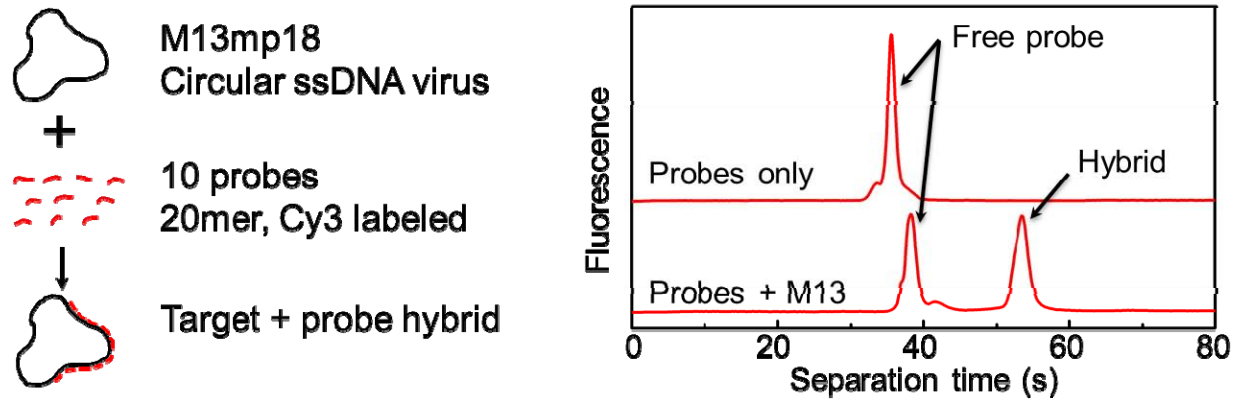

Figure 7: Proof-of-concept assay detecting M13mp18 virus by hybridization of dye-labeled oligonucleotide probes (up to 10 at a time) to viral DNA. The panel at right shows successful separation of "free" probe and target-bound probe ("hybrid"), along with a control reaction. The separation was obtained in a separation length of 22 mm, in 4 wt% polydimethylacrylamide (PDMA) separation matrix, following preconcentration for 2 minutes at 120 V/cm

3.1. Optimization of the separation

In principle, the separation of free probe (20mer) and target-bound probe (7249 base) should be easy. Initial attempts focused on using a polydimethylacrylamide (PDMA) sieving matrix at concentrations of 3-4%, which performed very well in initial experiments with separation of DNA ladders described in [6], and has also been successful as a sieving matrix for DNA sequencing separations [33]. With the hybridization assay, results with this matrix were not reproducible: sometimes successful separations were obtained, as in Figure 7 above, although the mobility shift of the hybrid peak was not always consistent, and sometimes the hybrid peak failed to appear. This may be due to the supercoiled circular nature of the target, which prohibits

the snake-like "reptation" mecihanism of DNA migration through a gel. The same target (M13mp18) when used as a template for dideoxy (Sanger) sequencing followed by capillary electrophoresis has been suspected of causing a variety of problems with injection [34-36].

Better results (meaning consistent recovery of the hybrid peak with a more reproducible migration time) were obtained using a sieving matrix consisting of Dextran (500,000 g/mol average molecular weight), 3.8 wt% in TTE buffer. Compared to the PDMA matrix, the Dextran solution is a very low-viscosity sieving matrix, easily introduced into the device by vacuum. Entanglement threshold concentration (c^*) for this polymer is about 1.2%, and typically sieving polymers are used at concentrations 5-10 times c^*. In this case, good results were found with a slightly lower concentration (~3-4 times c^*). The mechanism of separation may fall somewhere between a conventional "sieving" separation and a "transient entanglement" mechanism characteristic of polymer solutions below c^* [37]. Different results might be obtained for a linear (versus circular) or double-stranded (versus single stranded) target; some optimization of the sieving matrix may be necessary depending on the size and nature of the target.

Although most of the proof-of-concept work was done with off-chip hybridization, an interesting observation was made when trying to add salt to the running buffers to facilitate on-chip hybridization. Specifically, adding sodium chloride at a concentration of about 35 mM to the buffer reservoir "behind" the membrane was found to dramatically sharpen the free probe peak (data not shown here). There was apparently less effect on slower-migrating peaks. The mechanism is unclear, but I suspect that concentration polarization during preconcentration leads to a local increase buffer anions (mostly TAPS) in front of the membrane and depletion of salt from behind the membrane. Since salt is locally depleted on the other side of the membrane, there is (transiently) a shortage of current-carrying ions to cross the membrane upon injection. A "front" of increased salt concentration migrates down the separation channel, leading to a locally lower electric field, and consequently "destacking" of concentrated DNA bands as the migrate through this zone into a zone of lower conductivity and higher field. Adding some "fast" Cl^- ions on the back side of the membrane may amelioriate this by evening out conductivity gradients that develop during the injection process.

3.2. Improving limit of detection

As predicted by the detectability diagram (Figure 6), using multiple probes should improve detectability, over using a single probe. Thus, hybridization experiments were performed using 1, 2, 5, or 10 probes simultaneously targeting different regions of the M13mp18 template. These probes were designed to have similar length (20 bases), with similar GC contents (50%), and have melting temperatures (at 50 mM NaCl) ranging from 50-53 °C. 5 of the probes were labeled with Cy3 at the 5' end, and the rest were labeled with Cy3 at the 3' end. In general 5' labels were chosen by default, but 3' labels were used if the 5'-terminal base was "G", as there can be some G-dependent quenching of fluorophores.

Probe (10 nM final concentration of each probe) and template (~20 fmol per reaction) were mixed in a hybridization buffer containing 0.3M Na^+, 0.38M HEPES, pH 8.0. Reactions were denatured at 95°C for 5 minutes and immediately transferred to an incubator block at 46 °C 10

minutes. Samples were then diluted 1/10 for running on chip, with a 2 minute preconcentration (60 V/cm) followed by separation. The total assay time in this format is about 20 minutes.

As expected, increasing the number of probes increases the peak height of the hybrid peak, as seen in
Figure 8.

:

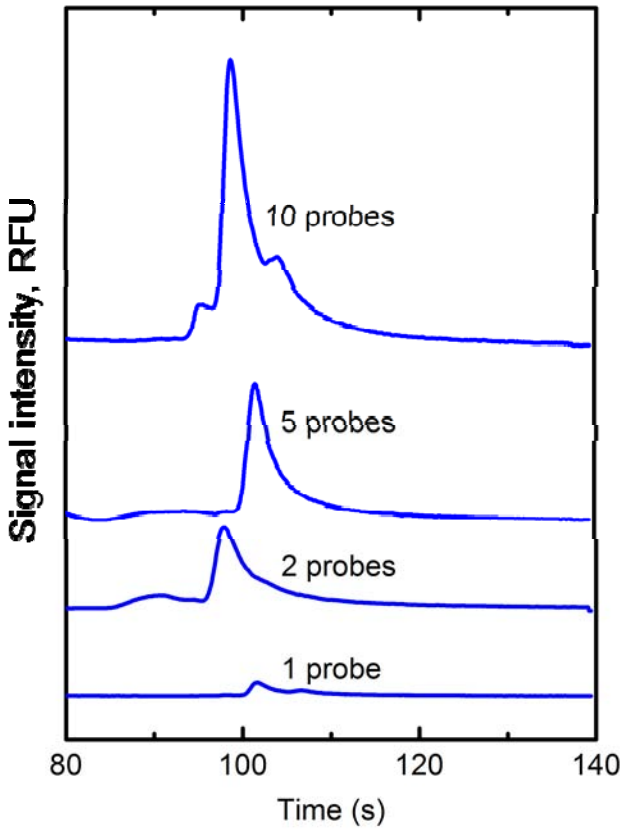

Figure 8: Effect of probe multiplicity on hybrid detection.

An increase in signal can also be obtained by increasing the preconcentration field or time. An example showing the effect of increasing preconcentration field is illustrated in Figure 9. Noteworthy in Figure 9 is that increasing the preconcentration field also dramatically increases the size of the probe peak. This phenomenon of course also occurs when increasing the number of probes (as in Figure 8, although the time scale in that figure is chosen to show only the hybrid peak). Although the resolution between the probe and hybrid peaks is quite good, overloading the device with "free" probe is not without consequence: the probe peak appears not to return to baseline, which would then impair the ability to discern a low-level hybrid peak. Furthermore, a very intense probe peak could temporarily "fatigue" the PMT and decrease response to a subsequent peak.

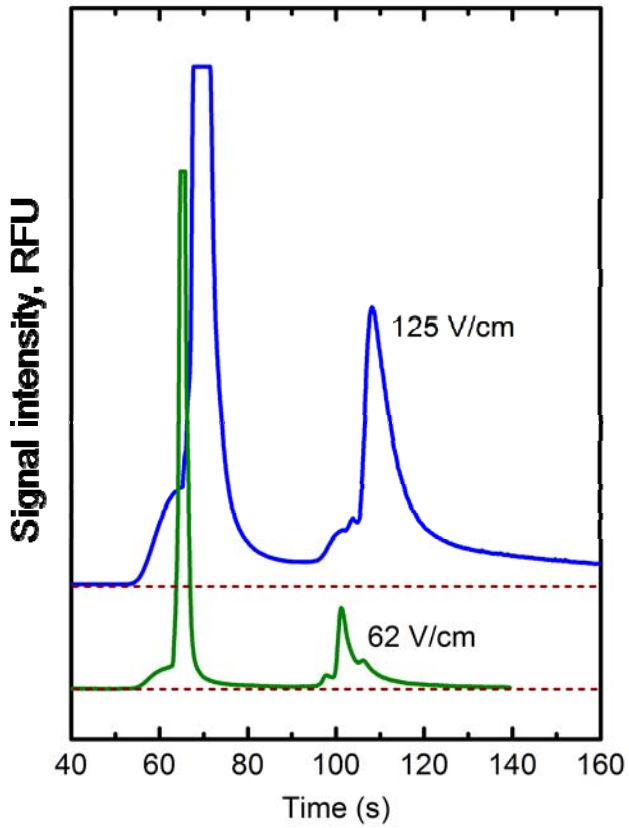

Figure 9: Increasing preconcentration field (2 minute duration) increases hybrid peak intensity, but with increased tailing of the free probe peak.

Given these concerns, it would be ideal to modify the assay to allow removal of unhybridized probe prior to the separation. One approach is to modify the membrane formulation, *i.e.* to a lower concentration of polyacrylamide that permits greater passage of the probe, while still retaining large targets. This is feasible; work performed with the µFlowFISH device demonstrated that probes easily pass a 10% polyacrylamide membrane, although the efficiency and biases of a new membrane formulation with respect to larger DNA targets remain to be determined (*i.e.* repeating the experiments performed for the 40% membrane described in reference [6]).

A second approach that was explored was enzymatic digestion of unhybridized probes. Several nucleases with different properties were tested for possible application, with partial success, although a detailed study was not completed at the time of this report. Briefly, nuclease options include:

- **S1 nuclease.** This is a single-strand-specific *endonuclease*. In the case of the single-stranded circular M13 target, this nuclease will degrade any unhybridized probe, as well as any single-stranded regions of the target not bound to a probe. If the digestion goes to completion, the reaction products would thus be a set of dye-labeled 20mer duplexes (essentially the regions of the target "protected" by the probes), and mononucleotides. The enzyme is quite robust and thermally stable, although too large of an excess of

enzyme can result in indiscriminate digestion of DNA. The buffer requirements do require some consideration: the enzyme is tolerant to fairly high salt concentrations (up to ~300 mM), but does require zinc ions which, like Mg^{++}, can presumably impact hybridization stringency and kinetics. The optimal pH for the reaction is 4.6, which is outside the range attainable with typical "good" anions for electrophoresis, and would necessitate buffering with a faster anion such as acetate. If we are to perform hybridization and digestion in the same buffer, there is also a possible concern for depurination of DNA during the denaturing step, due to elevated temperature at low pH. This use of S1 nuclease is analogous to the "nuclease protection assay" which is commonly used to detect RNA targets (frequently using radioactivity) [38]. Combining the S1 nuclease digestion with membrane concentration and separation is a novel approach to miniaturizing and automating this standard laboratory technique using fluorescence detection.

- **Exonuclease I**. This is an *exonuclease* that is highly specific for single-stranded DNA, and digests from the 3' end, requiring a 3' hydroxyl. Tests have shown that it is also active on our 3'-dye-labeled probes, although more slowly than on our 5'-labeled probes. If the digestion goes to completion, the reaction products would be the intact single-stranded circular target with hybridized probes, and mononucleotides. The enzyme does require addition of Mg^{++}, but is otherwise tolerant of a wide variety of buffer conditions around pH 7-8, and does retain some activity at 45 °C, allowing digestion to be performed at a higher stringency than the recommended temperature for the enzyme (37 °C). The digestion appears to be effective at greatly reducing unhybridized probes, but in the 3.8% Dextran matrix, some labeled product (possibly dye-labeled mononucleotides) co-migrate close to the expected time for the hybrid peak. In some instances, an additional product leads to an elevated baseline toward the end of the run; this might be attributed to small dye-labeled digestion products that migrate into the membrane, and then slowly migrate out when the field is reversed. These artifacts would need to be resolved (perhaps by changing the formulation of the sieving matrix) prior to proceeding with this enzyme.

- **Exonuclease VII.** This is another *exonuclease* with high specificity for ssDNA. As with Exo I, the products with the single-stranded circular template would be intact target with hybridized probes, and digestion products from the probes (mono- and small oligonucleotides, including dye-labeled products). Two features make Exo VII an attractive alternative to Exo I for this application. First, digestion proceeds from both 3'- and 5'- termini, meaning there is no concern as to which end is dye-labeled. Second, the reaction does not require any divalent cations and retains partial activity at temperatures in excess of 40 °C, meaning there is no concern with altering stringency to accommodate the enzyme. The enzyme is tolerant of high concentrations of monovalent cations. Combining digestion with a hybridization reaction was only attempted once; results suggested only partial removal of excess probe, but without noticeable co-migration of reaction products as with Exonuclease I. Literature search on additional properties of the enzyme indicate that it requires phosphate in the digestion buffer [39], which was not included on the first test; additional work can explore whether simple addition of phosphate to the reaction buffer can improve performance of this enzyme.

Although promising for removing excess probe, these enzymatic digestion steps do remove the "enzyme-free" feature that drove exploration of the assay in the first place. Compared to PCR, the nuclease enzymes are quite robust (thermally stable and resistant to inhibitors), and might be amenable to greater thermal stabilization through formulation with simple additives such as trehalose or Dextran.

To date, the best sensitivity obtained (without any enzymatic digestion) has been 400 amol of M13mp18 template loaded into the device. As illustrated in Figure 10 this was achieved with good signal-to-noise (~ 20) using a standard "mild" preconcentration (120s at 60 V/cm), suggesting there is substantial room for increasing detection limits, particularly if the difficulties associated with a large probe peak can be solved.

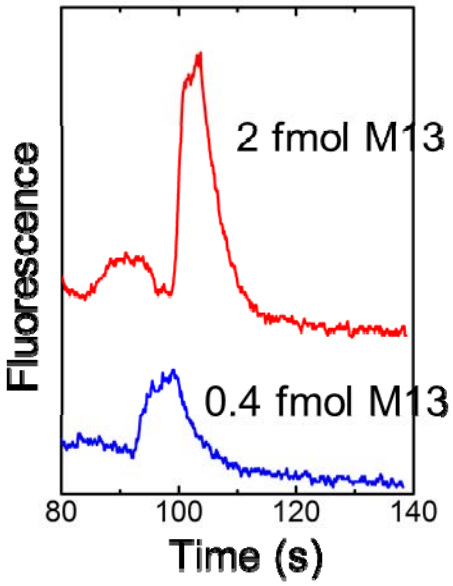

Figure 10: Sensitivity for low concentrations of M13mp18 (using 10 probes).

400 amol is still a relatively high copy number for pathogens in clinical samples, and thus at this level of sensitivity the assay is unlikely to compete with PCR. Further reduction in the sample volume loaded on the chip (*i.e.* by re-designing the chip manifold with smaller holes, and smaller electrodes to work with ~5 μL instead of the current 80 μL) would immediately reduce the detection limits by an order of magnitude. Solving the problem of primer peak "tailing" after extensive preconcentration, whether by enzymatic digestion or reformulation of the membrane, would allow more aggressive preconcentration, perhaps allowing an additional order of magnitude of sensitivity. The LIF detection is relatively well optimized, although further gains might be achieved using a more sensitive or less noisy PMT, for example.

4. USE OF MEMBRANE PRECONCENTRATION DEVICE FOR DETECTING DRUG RESISTANCE GENES

The membrane preconcentration chip is useful for any application requiring highly sensitive size-based separation of DNA. Besides the amplification-free hybridization assay discussed thus far, the chip is also useful for separating products from a conventional PCR reaction, for example in diagnostics. One example that was explored is multiplex PCR for detection of horizontally transferred drug resistance genes.

4.1. Background

Klebsiella pneumoniae and other Gram-negative bacteria with genes encoding carbapenemases such as KPC or New Delhi metallo-b-lactamase (NDM-1) are potentially a grave concern for public health. Carbapenems (imipenem, *etc*) are drugs of last resort for Gram-negative pathogens [40-42]. Besides coding for resistance to these drugs, carbapenemase genes frequently reside on highly transmissible plasmids simultaneously coding for resistance to numerous other classes of antibiotics, leading to infections that are highly intractable to treatment.

Carbapenamases can be difficult to detect by susceptibility testing methods, and we are developing rapid genetic (PCR) tests for these resistance genes, using novel instrumentation designed for limited-resource settings. Genetic tests also have drawbacks: they may miss novel sequence variants, and may pick up non-functional or non-expressed genes, and are usually limited to detecting a few common genes per test.

Real-time PCR tests are popular in clinical settings due to the relative simplicity of amplification plus detection in a single tube, although real-time tests have more limited multiplexing ability. Multiplex PCR with amplicon sizing can detect more targets per reaction, but require extra work to transfer samples to a gel for analysis. Instrumentation developed in this project (membrane preconcentration chip) along with other projects (rapid PCR "wheel", DNA extraction) allows automation of sample prep, amplification, and analysis allowing rapid, high-sensitivity analysis of amplicons. In this work, we test components of this system for a small panel of carbapenemase genes, with the ultimate goal of performing rapid, multiplexed detection of a large panel of drug resistance genes directly in a clinical setting.

4.2 Methods

As a first step toward applying our instrumentation to detecting carbapenemase genes, we have tested a small panel of strains with a low-level multiplex PCR for $bla_{\text{NDM-1}}$, bla_{KPC}, and Enterobacteriaceae 16S gene (internal control). The degree of multiplexing was limited primarily by the strains we had available for testing, rather than an inherent limitation of the technology.

Table 2: Primers used for detecting carbapenemase genes

Primer name	Sequence	Amplicon size (bp)	Ref.
NDM-GBM-F	CCCGGCCACACCAGTGACA	129	[43]
NDM-GBM-R	GTAGTGCTCAGTGTCGGCAT		
MultiKPC_for	CATTCAAGGGCTTTCTTGCTGC	538	[44]
MultiKPC_rev	ACGACGGCATAGTCATTTGC		
ENT-F (16S)	GTTGTAAAGCACTTTCAGTGGTGAGGAAGG	424	[45]
ENT-R (16S)	GCCTCAAGGGCACAACCTCCAAG		
DG74 (16S)	AGGAGGTGATCCAACCGCA	370	[46]
RW01 (16S)	AACTGGAGGAAGGTGGGGAT		

We obtained purified DNA from the following ATCC control strains:

Table 3: Strains used for testing PCR assay

ATCC Strain	Comments
K. Pneumoniae BAA-1705	KPC positive control for modifiied Hodge test (MHT)
K. Pneumoniae BAA-1706	Negative control strain for modified Hodge test
K. Pneumoniae BAA-2146	Multi-drug resistant; bla_{KPC} negative, bla_{NDM-1} positive

We optimized a "conventional" multiplex PCR reaction for these primers and these strains. Final conditions were [pmol/µL] each primer, 57 C annealing temperature, 1 ng template DNA in a 25 µL reaction. As a positive control for amplification, we used either a "universal" 16S primer set (DG74 + RW01), or the "ENT" 16S primer set. This set targets most Enterobacteriaceae and Vibrioaceae but is less sensitive to contamination than "universal" 16S primers. We obtained positive amplification in 30 cycles from 50-500 pg of bacterial genomic DNA in a 25 µL reaction.

4.3 Results

4.3.1 Multiplex PCR optimization

Conventional PCR thermocycling with agarose gel electrophoresis allowed detection of expected bands for each strain, as shown below.

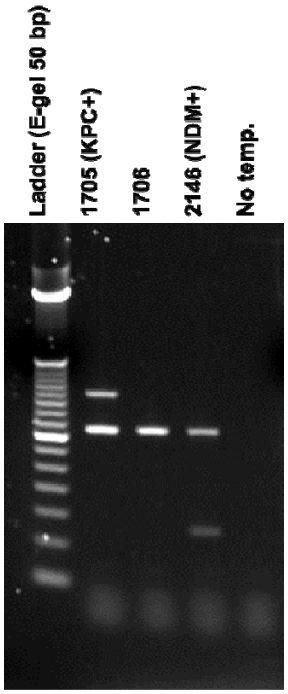

Figure 11: 2% Agarose + EtBr gel image of carbapenemase multiplex with "universal" 16S primer control, showing expected bands at 129, 370, and 538 bp. The 50 bp ladder (far left lane) has bands at 50, 100, 150, etc. The "bright" ladder bands represent 350 bp and 800 bp.

The same set of primers (either the same ratio of primers, or a rebalanced mixture) was tested using the "PCR wheel" for rapid thermal cycling; all bands could be detected with the PCR but the relative abundance of primers requires further optimization. Bands on the agarose gel for primer mix 2 appear "smeared" due to insufficient dilution prior to loading on the gel.

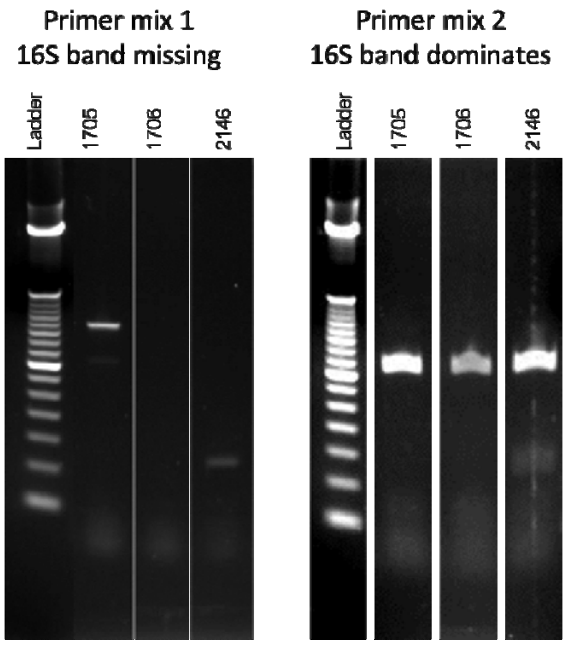

Figure 12: Agarose gel electrophoresis showing products from carbapenemase multiplex PCR with PCR wheel for rapid thermal cycling. Primer mix 1 (same as in Figure 11) shows the expected bands for NDM-1 and KPC. A re-balanced primer mix (Mix 2) which results in overproduction of the 16S amplification control band and apparent loss of the KPC band. Further optimization is required.

4.3.2 Membrane preconcentration chip for detection of amplicons

For detection using the membrane preconcentration chip, we used conditions similar to those developed when testing the rates and biases of preconcentration [6], with two changes. (1) The sieving matrix was 4% PDMA rather than 5% PDMA, and (2) an "on-column" labeling protocol was used, rather than dye-labeled primers. On-column detection allows use of simple, inexpensive unlabeled primers and DNA ladders, although it would limit the possibility for spectral multiplexing.

Results of the chip-based detection for a size ladder and the multiplex PCR are shown in Figure 13. A quantitative ladder was used, allowing comparison of peak area as a function of DNA size. The on-column labeling strategy showed a linear correlation between fragment mass and peak area. This is a good result, and was not entirely expected: because the dye used for on-column labeling is itself positively charged, it was possible that there would be some size-dependent labeling artifacts associated with the dye concentrating (or not concentrating) near the membrane. Good separation was observed for the ladder peaks between 100 and 800 bp. The 2000 bp peak was baseline resolved, but examination of mobility versus size (plot in upper right corner of Figure 13) indicates that the 2000 bp peak lies outside the region of good sieving behavior (linear dependence of log(mobility) vs log(size)).

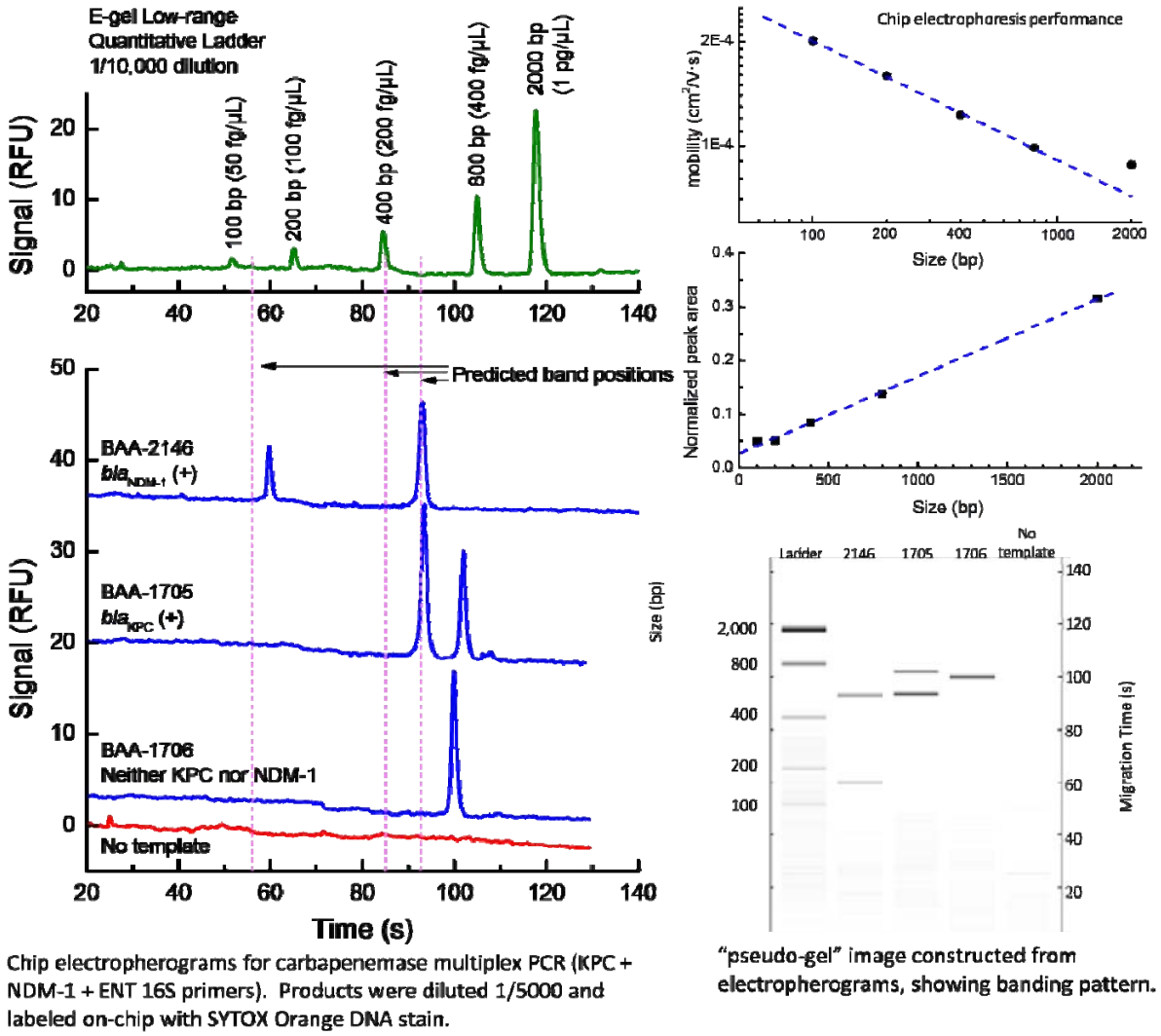

Chip electropherograms for carbapenemase multiplex PCR (KPC + NDM-1 + ENT 16S primers). Products were diluted 1/5000 and labeled on-chip with SYTOX Orange DNA stain.

"pseudo-gel" image constructed from electropherograms, showing banding pattern.

Figure 13: Membrane preconcentration chip for analysis of carbapenemase multiplex PCR, with control separation of a quantitative DNA ladder, and quantitative metrics of ladder separation.

Chip electrophoresis gives the same banding pattern as the traditional gel, but the migration times are shifted from the expected position, because many runs (>20) were performed sequentially without replacing buffers or sieving polymer, causing a gradual slowing of migration. One solution is to include leading & trailing "reference bands" to tie each run to the size standard. This is a standard approach with chip and capillary electrophoresis, *e.g.* the Agilent Bioanalyzer.

As discussed below, the absolute sensitivity of detection with the membrane preconcentration chip exceeds by orders of magnitude that which can be obtained by slab gel electrophoresis or the Agilent Bioanalyzer, in an order of magnitude shorter time than can be obtained by capillary electrophoresis. The analyses shown in Figure 13 were obtained with PCR products diluted 1/5000. It is likely that products could still be detected in as few as 15-20 PCR cycles, with lower dilution of the product, potentially reducing the time required for detection.

4.3.3 Optimization of on-chip labeling technique

For on-column labeling, we used the intercalating dye SYTOX Orange, which is a good match for the 532-nm laser with 570-610 nm bandpass detection and has been used previously for CE and chip separations of DNA [47]. This dye was included in the separation matrix, and in the "run waste" reservoir (at the end of the separation channel). Like most intercalators, SYTOX Orange is positively charged, and thus migrates counter to the direction of DNA migration, allowing fragments to be labeled as they migrate down the separation channel. Unlike the cyanine dimer dyes (YOYO, POPO, *etc*) which can bind "permanently", SYTOX Orange equilibrates with DNA relatively quickly [48], meaning that if free dye is not present in the sieving matrix or running buffer, the DNA becomes "unstained".

Some optimization of the on-column labeling protocol was required. During the "pre-run" steps (preconcentration, *etc*), the "free" dye in the separation channel (present at about 500 nM), as well as dye which adsorbs to the microchannel surface, gives some background fluorescence (the unincorporated dye has small but non-negligible fluorescence). Since the dye is stationary (there is no current in the separation channel during these steps), the dye photobleaches, resulting in a decrease in the fluorescence signal. Upon switching the direction of the electric field, free dye begins to migrate "up" the separation channel, causing the background signal to increase slowly. I suspect that the slow increase is due to establishment of an equilibrium between dye in solution and dye adsorbed to the surface (fresh dye is displacing previously bound, photobleached dye). The slow increase in baseline often persists during the period when DNA peaks are migrating past the detector. This is not strictly a problem for detection, but could be problematic for quantitation, and in any event is non-ideal.

The rate of increase as well as the equilibrium level of the baseline was found to depend on the current in the separation arm (perhaps reflecting the rate at which fresh dye is brought into the detection region, and thus the availability of fresh dye to displace bleached dye from the surface). Using the current-control capabilities of the power supply, it was possible to apply current in the separation channel during the pre-run which matches the current during the separation step. This allows an "equilibrium" baseline to be established during the pre-run, and allows the detection DNA peaks on a more ideal, horizontal baseline.

Tight binding of SYTOX Orange to microchannel surfaces has been reported previously [48], and it seems to be difficult to avoid despite coating of surfaces to mask positive charges. Other dyes might be explored to avoid this problem; if the problem is truly due to surface-bound dye, it is also possible that an optimized confocal pinhole will allow better rejection of fluorescence at the top and bottom surfaces of the channel, as opposed the laser focus at the center of the channel.

Even with the high background associated with SYTOX Orange, very high sensitivity was obtained: the ladder separations show easy detection of the ladder peak at 50 fg/μL, and other runs at higher dilution showed this peak could be detected down to 20 fg/μL (not shown). These results were obtained at relatively low setting of PMT gain (to allow on-scale detection of all peaks in the ladder), and with a "mild" preconcentration (2 minutes at 60 V/cm) meaning we can

likely detect substantially lower concentrations of DNA with relatively minor tweaks to the system. The current results are approximately 2 orders of magnitude better than the best sensitivity claimed for the Agilent Bioanalyzer, and within an order of magnitude of results claimed as "ultra-sensitive" LIF detection using intercalating dyes in CE (~ 1-10 fg/μL) [49]. For sake of reference, 1 fg represents about 12×10^6 molecules of a 50-bp DNA, or 300×10^3 molecules of 2000-bp DNA. Thus, on-chip labeling with membrane preconcentration appears to put us within reach of directly detecting DNA with copy number <1 million.

4.4 Multiplex PCR Conclusion and Future Work

The results show successful transition of a conventional, low-throughput multiplex PCR with gel electrophoresis to two platforms amenable to automation (1) rapid cycle PCR using Sandia's patent-pending "PCR Wheel", and (2) rapid, ultra-sensitive chip electrophoresis. Together, these technologies will allow PCR detection with small reaction volume and fewer cycles in a shorter total assay time. Further development of the chip electrophoresis is needed to tighten up the migration times and further increase sensitivity with on-chip labeling. The low power rapid thermal cycler with integrated sample prep will enable operations in limited resource settings (hospital/point-of-care). For clinical use the drug resistance multiplex should be expanded, but this requires validation against a larger collection of isolates.

5. CONCLUSIONS

Work thus far provides proof-of-concept for direct detection of $<10^9$ copies of a pathogen nucleic acid sequence by hybridization followed by electrophoretic separation with LIF detection, with membrane preconcentration allowing more sensitive detection of target-bound probes. Further improvements to chip design (*e.g.* the ability to load smaller volumes into the on-chip reservoirs; membrane formulation to allow selective passage of probes), as well as improvements to detection optics, can potentially provide 1-2 orders of magnitude of additional improvement in detection limits.

The main advantages of the direct hybridization assay are speed and simplicity. The only operations required are mixing of target, probe, and buffer solutions, and a simple temperature program involving denaturation at 95 °C for five minutes, followed by incubation at 45-50 °C for 5-10 additional minutes. The electrophoretic analysis step requires approximately 5 minutes, giving the assay a total run time of about 15 minutes. Hardware has already been designed at Sandia for portable operation of microfluidic electrophoresis chips as well as hands-free handling and thermal cycling of microliter-scale volumes of fluids, and thus this assay could be integrated into existing systems for portable operation.

The main disadvantage for the assay is its relatively poor sensitivity, relative to PCR. 10^9 (or 10^7, with improvements) is a high copy number for most pathogens in clinical samples. Even with improvements, the direct hybridization assay is unlikely to compete with PCR, LAMP, or other amplification-based techniques that can detect targets at <10 copies per sample. With relatively high detection limits, the hybridization assay would need to be coupled to a process for extraction and concentration of nucleic acids from large-volume samples, or to a "natural" amplification process such as culture (which is time consuming). Meanwhile, recent developments in PCR have made inhibitors less of a problem for robust, fieldable PCR: mutant polymerases such as KlenTaq are now available that are resistant to common sources of inhibition (*e.g.* in blood) [50]. Several commercial vendors such as EvoPrep and ZyGem now offer simple, one-step extraction kits that are both easy to use and inactivate common inhibitors. PCR remains dependent upon a cold chain, although several studies now suggest that simple additives such as trehalose can stabilize a PCR reaction mixture in lyophilized form for weeks or months at room temperature. With these advances, PCR as well as isothermal amplification methods such as LAMP are likely to find increased success as "fieldable" techniques for portable diagnostics.

In the course of developing and testing the hybridization assay, the membrane preconcentration chip has proved valuable for detecting very low concentrations of DNA. In terms of absolute senstitivity, the membrane preconcentration process allows detection of much lower concentrations of input DNA than a "conventional" microchip electrophoresis device such as the Agilent Bioanalyzer, and several orders of magnitude lower concentration than slab gel electrophoresis. The speed and resolution of separation is comparable to that seen with other chip electrophoresis devices like the Bioanalyzer, but the sensitivity of detection is comparable to that obtained with highly optimized capillary electrophoresis, which is orders of magnitude slower. Additionally, CE requires extensively desalted samples to achieve high sensitivity, whereas the membrane preconcentration device is relatively tolerant to millimolar concentrations

of "fast" ions such as Cl^- in the sample. The desirable properties of the membrane preconcentration device allowed it to be used in this work to enable a highly sensitive multiplex PCR-based detection of bacterial drug resistance genes, and could potentially be incorporated into a variety of rapid, portable diagnostic platforms.

Extensive experiments with DNA preconcentration has shown that uncharged membranes are preferable to negatively charged membranes for most applications, allowing faster preconcentration and better separations following preconcentration. Negative membranes allow more effective preconcentration of very small, negatively charged analytes such as oligonucleotides, but display a higher degree of ion concentration polarization, which negatively impacts several aspects of operation [6].

6. REFERENCES

[1] Nkodo, A. E., Garnier, J. M., Tinland, B., Ren, H. J., Desruisseaux, C., McCorm ick, L. C., Drouin, G., Slater, G. W., "Diffusion Coefficient of DNA Molecules During Free Solution Electrophoresis", *Electrophoresis* 2001, *22*, 2424-2432.

[2] Hatch, A. V., Herr, A. E ., Throckmorton, D. J., Brennan, J. S., Si ngh, A. K., "Integrated Preconcentration Sds-Page of Proteins in Microchips Using Photopatterned Cross-Linked Polyacrylamide Gels", *Anal. Chem.* 2006, *78*, 4976-4984.

[3] Hecht, A. H., Sommer, G. J., Durland, R. H., Yang, X. B., Singh, A. K., Hatch, A. V., "Aptamers as Affinity Reag ents in an Integrated E lectrophoretic Lab-on-a-Chip Platform", *Anal. Chem.* 2010, *82*, 8813-8820.

[4] Herr, A. E., Hatch, A. V., Throckm orton, D. J., Tran, H. M., Brennan, J. S., Giannobile, W. V., Singh, A. K., "Microfluidic Imm unoassays as Rapid Saliva-Based Clinical Diagnostics", *Proc. Natl. Acad. Sci. USA* 2007, *104*, 5268-5273.

[5] Meagher, R. J., Hatch, A. V., Renz i, R. F., Singh, A. K., " An Integrated Microfluidic Platform for Sensitive and Rapid Detection of Biological Toxins", *Lab Chip* 2008, *8*, 2046-2053.

[6] Meagher, R. J., Thaitrong, N., "Mic rochip Electrophoresis of DNA Following Preconcentration at Ph otopatterned Gel Mem branes", *Electrophoresis* 2012, *33*, 1236-1246.

[7] Wetmur, J. G., "DNA Probes - Applicati ons of the Princip les of Nucleic-Acid Hybridization", *Critical Reviews in Biochemistry and Molecular Biology* 1991, *26*, 227-259.

[8] Owczarzy, R., Moreira, B. G., You, Y., Be hlke, M. A., W alder, J. A., "Predictin g Stability of DNA Du plexes in Solutions Containing Magnesium and Monovalent Cations", *Biochemistry* 2008, *47*, 5336-5353.

[9] Owczarzy, R., Tataurov, A. V., Wu, Y., Manthey, J. A., McQuisten, K. A., Almabrazi, H. G., Pedersen, K. F., Lin, Y., Garretson, J., Mc Entaggart, N. O., Sailor, C. A., Dawson, R. B., Peek, A. S., "Idt Scitools: A Suite for Analysis and Design of Nucleic Acid Oligomers", *Nucleic Acids Research* 2008, *36*, W163-W169.

[10] Yilmaz, L. S., Parnerkar, S., Noguera , D. R., "Mathfish, a W eb Tool That Uses Thermodynamics-Based Mathematical Models for in Silico Evaluation of Oligonucleotide Probes for Fluorescen ce in Situ Hybridization", *Appl. Environ. Microbiol.* 2011, *77*, 1118-1122.

[11] Stellwagen, E., Muse, J. M., Stellw agen, N. C., "Monovalent Cation Size and DNA Conformational Stability", *Biochemistry* 2011, *50*, 3084-3094.

[12] Meagher, R. J., Won, J. I., McCormick, L. C., Nedelcu, S., Bertrand, M. M., Bertram, J. L., Drouin, G., Barron, A. E., Slater, G. W ., "End-Labeled Free-Solution Electrophoresis of DNA", *Electrophoresis* 2005, *26*, 331-350.

[13] Donnan, F. G., "Theory of Membrane Equilibria and Membrane-Potentials in the Presence of Non-Dialyzing Electrolytes - a Contribution to Physical-Chemical Physiology (Reprinted from Zeitshrift Fur Elektrochemie Und Angewandte Physikalische Chemie, Vol 17, Pg 572, 1911)", *Journal of Membrane Science* 1995, *100*, 45-55.

[14] Block, M., Kitchene.Ja, "Polarization Phenomena in Commercial Ion-Exchange Membranes", *Journal of the Electrochemical Society* 1966, *113*, 947-&.

[15] Ohshima, H., Kondo, T., "Relationship among the Surface-Potential, Donnan Potential and Charge-Density of Ion-Penetrable Membranes", *Biophysical Chemistry* 1990, *38*, 117-122.

[16] Dhopeshwarkar, R., Crooks, R. M., Hlushkou, D., Tallarek, U., "Transient Effects on Microchannel Electrokinetic Filtering with an Ion-Permselective Membrane", *Anal. Chem.* 2008, *80*, 1039-1048.

[17] Hlushkou, D., Dhopeshwarkar, R., Crooks, R. M., Tallarek, U., "The Influence of Membrane Ion-Permselectivity on Electrokinetic Concentration Enrichment in Membrane-Based Preconcentration Units", *Lab Chip* 2008, *8*, 1153-1162.

[18] Hoeltzel, A., Tallarek, U., "Ionic Conductance of Nanopores in Microscale Analysis Systems: Where Microfluldics Meets Nanofluidics", *J. Sep. Sci.* 2007, *30*, 1398-1419.

[19] Kuo, C. H., Wang, J. H., Lee, G. B., "A Microfabricated Ce Chip for DNA Pre-Concentration and Separation Utilizing a Normally Closed Valve", *Electrophoresis* 2009, *30*, 3228-3235.

[20] Wang, L. H., Liu, D. Y., Chen, H., Zhou, X. M., "A Simple and Sensitive Transient Itp Method for on-Chip Analysis of Pcr Samples", *Electrophoresis* 2008, *29*, 4976-4983.

[21] Mani, A., Zangle, T. A., Santiago, J. G., "On the Propagation of Concentration Polarization from Microchannel-Nanochannel Interfaces Part I: Analytical Model and Characteristic Analysis", *Langmuir* 2009, *25*, 3898-3908.

[22] Zangle, T. A., Mani, A., Santiago, J. G., "On the Propagation of Concentration Polarization from Microchannel-Nanochannel Interfaces Part Ii: Numerical and Experimental Study", *Langmuir* 2009, *25*, 3909-3916.

[23] Zangle, T. A., Mani, A., Santiago, J. G., "Theory and Experiments of Concentration Polarization and Ion Focusing at Microchannel and Nanochannel Interfaces", *Chem. Soc. Rev.* 2010, *39*, 1014-1035.

[24] Jian, W., Ugaz, V. M., "Using in Situ Rh eology to Chara cterize the Micros tructure in Photopolymerized Polyacrylamide Gels for DNA Electrophoresis", *Electrophoresis* 2006, *27*, 3349-33583358.

[25] Holmes, D. L., Stellwagen, N. C., "Es timation of Polyacrylamide-Gel Pore-Size f rom Ferguson Plots of Linear DNA Fragm ents .2. Co mparison of Gels with Different Cross-Linker Concentrations, Added Agarose and Added Linear Polyacrylamide", *Electrophoresis* 1991, *12*, 612-619.

[26] Holmes, D. L., Stellwagen, N. C., "Es timation of Polyacrylamide-Gel Pore-Size f rom Ferguson Plots of Norm al and Ano malously Migrating DNA Frag ments .1. Gels Containing 3-Percent N,N'-Methylenebisacrylamide", *Electrophoresis* 1991, *12*, 253-263.

[27] Stellwagen, N. C., "Apparent Pore Size of Polyacrylamide Gels: Comparison of Gels Cast and Run in Tris-Acetate-Edt a and Tris-Borate-Edta Buffers", *Electrophoresis* 1998, *19*, 1542-1547.

[28] Tsong-Pin, H., Cohen, C., "Observations on the Structure of a Polyacrylam ide Gel from Electron Micrographs", *Polymer* 1984, *25*, 1419-1423.

[29] Kirby, B. J., W heeler, A. R., Zare, R. N ., Fruetel, J. A., Shepodd, T. J., "Programmable Modification of Cell Adhesion and Zeta Potential in Silica Microchips", *Lab Chip* 2003, *3*, 5-10.

[30] Verkman, A. S., "Developm ent and Biol ogical Applications of Chloride-Sensitive Fluorescent Indicators", *American Journal of Physiology* 1990, *259*, C375-C388.

[31] Orosz, D. E., Garlid, K. D., "A Sens itive New Fluorescence Assay for Measuring Proton Transport across Liposomal Membranes", *Anal. Biochem.* 1993, *210*, 7-15.

[32] Liu, P., Meagher, R. J., Light, Y. K., Yilmaz, S., Chakraborty, R., Arkin, A. P., Hazen, T. C., Singh, A. K., "Microfluidic Fluorescence in Situ Hybridization and Flow Cytometry (Mu Flowfish)", *Lab Chip* 2011, *11*, 2673-2679.

[33] Fredlake, C. P., Hert, D. G., Kan, C. W., Chiesl, T. N., Root, B. E., Forster, R. E., Barron, A. E., "Ultrafast DNA Sequencing on a Micr ochip by a Hybrid Separation Mechanis m That Gives 600 Bases in 6.5 Minutes", *Proc. Natl. Acad. Sci. USA* 2008, *105*, 476-481.

[34] Swerdlow, H., Dewjager, K. E., Brady, K ., Grey, R., Dovichi, N. J., Gesteland, R., "Stability of Capillary Gels for Automated Sequencing of DNA", *Electrophoresis* 1992, *13*, 475-483.

[35] Ruiz-Martinez, M. C., Sa las-Solano, O., Carrilho, E., Kotler, L., Karger, B. L., "A Sample Purification Method for R ugged and High-Performance DNA Sequencing by

Capillary Electrophoresis Using Replaceable Polymer Solutions. A. Development of the Cleanup Protocol", *Anal. Chem.* 1998, *70*, 1516-1527.

[36] Salas-Solano, O., Ruiz-Martinez, M. C., Carrilho, E., Kotler, L., Karger, B. L., "A Sample Purification Method for Rugged and High-Performance DNA Sequencing by Capillary Electrophoresis Using Replaceable Polymer Solutions. B. Quantitative Determination of the Role of Sample Matrix Components on Sequencing Analysis", *Anal. Chem.* 1998, *70*, 1528-1535.

[37] Barron, A. E., Blanch, H. W., Soane, D. S., "A Transient Entanglement Coupling Mechanism for DNA Separation by Capillary Electrophoresis in Ultradilute Polymer-Solutions", *Electrophoresis* 1994, *15*, 597-615.

[38] Bach, R., Grummt, I., Allet, B., "The Nucleotide-Sequence of the Initiation Region of the Ribosomal Transcription Unit from Mouse", *Nucleic Acids Research* 1981, *9*, 1559-1569.

[39] Chase, J. W., Richards.Cc, "Exonuclease Vii of Escherichia-Coli - Purification and Properties", *Journal of Biological Chemistry* 1974, *249*, 4545-4552.

[40] Nordmann, P., Cuzon, G., Naas, T., "The Real Threat of Klebsiella Pneumoniae Carbapenemase-Producing Bacteria", *Lancet Infectious Diseases* 2009, *9*, 228-236.

[41] Nordmann, P., Dortet, L., Poirel, L., "Carbapenem Resistance in Enterobacteriaceae: Here Is the Storm!", *Trends in Molecular Medicine* 2012, *18*, 263-272.

[42] Nordmann, P., Poirel, L., Walsh, T. R., Livermore, D. M., "The Emerging Ndm Carbapenemases", *Trends in Microbiology* 2011, *19*, 588-595.

[43] Voets, G. M., Fluit, A. C., Scharringa, J., Stuart, J. C., Leverstein-van Hall, M. A., "A Set of Multiplex Pcrs for Genotypic Detection of Extended-Spectrum Beta-Lactamases, Carbapenemases, Plasmid-Mediated Ampc Beta-Lactamases and Oxa Beta-Lactamases", *International Journal of Antimicrobial Agents* 2011, *37*, 356-359.

[44] Dallenne, C., Da Costa, A., Decre, D., Favier, C., Arlet, G., "Development of a Set of Multiplex Pcr Assays for the Detection of Genes Encoding Important Beta-Lactamases in Enterobacteriaceae", *Journal of Antimicrobial Chemotherapy* 2010, *65*, 490-495.

[45] Nakano, S., Kobayashi, T., Funabiki, K., Matsumura, A., Nagao, Y., Yamada, T., "Development of a Pcr Assay for Detection of Enterobacteriaceae in Foods", *Journal of Food Protection* 2003, *66*, 1798-1804.

[46] Greisen, K., Loeffelholz, M., Purohit, A., Leong, D., "Pcr Primers and Probes for the 16s Ribosomal-Rna Gene of Most Species of Pathogenic Bacteria, Including Bacteria Found in Cerebrospinal-Fluid", *Journal of Clinical Microbiology* 1994, *32*, 335-351.

[47] Yan, X. M., Hang, W ., Majidi, V., Marrone , B. L., Yoshida, T. M., "Evaluation of Different Nucleic Acid Stains for Sens itive Double-Stranded DNA Analysis with Capillary Electrophoretic Separation", *Journal of Chromatography A* 2002, *943*, 275-285.

[48] Yan, X. M., Habbersett, R. C., Yos hida, T. M., Nolan, J. P., Jett, J. H., Marrone, B . L., "Probing the Kinetics of Sytox Orange Stain Binding to Double-Stranded DNA with Implications for DNA Analysis", *Anal. Chem.* 2005, *77*, 3554-3562.

[49] Zhu, H. P., Clark, S. M., Benson, S. C., Rye, H. S., Glazer, A. N., Mathies, R. A., "High-Sensitivity Capillary E lectrophoresis of Double-Str anded DNA Fragm ents Using Monomeric and Dim eric Fluorescent Intercalating Dyes", *Anal. Chem.* 1994, *66*, 1941-1948.

[50] Zhang, Z., Kermekchiev, M. B., Barnes, W. M., "Direct DNA Am plification from Crude Clinical Samples Using a Pcr Enhancer Cocktail and Novel Mutants of Taq", *J. Mol. Diagn.* 2010, *12*, 152-161.

DISTRIBUTION

1	MS0359	D. Chavez, LDRD Office	1911
1	MS0899	Technical Library	9536 (electronic copy)
1	MS9291	Anup Singh	8620
1	MS9291	Robert Meagher	8621


Sandia National Laboratories